molecules

MDPI

Article

Interfacial Properties, Wettability Alteration and Emulsification Properties of an Organic Alkali–Surface Active Ionic Liquid System: Implications for Enhanced Oil Recovery

Bennet Nii Tackie-Otoo [1,2,*], Mohammed Abdalla Ayoub Mohammed [1,2,*], Hazman Akmal Bin Mohd Zalghani [1], Anas M. Hassan [3], Pearl Isabellah Murungi [1] and Grace Amabel Tabaaza [4]

[1] Petroleum Engineering Department, Universiti Teknologi PETRONAS, Seri Iskandar 32610, Malaysia; hazman.akmal_24316@utp.edu.my (H.A.B.M.Z.); pearl_20001549@utp.edu.my (P.I.M.)
[2] Centre of Research in Enhanced Oil Recovery, Universiti Teknologi PETRONAS, Seri Iskandar 32610, Malaysia
[3] Petroleum Engineering Department, Khalifa University of Science, Technology and Research, Abu Dhabi P.O. Box 127788, United Arab Emirates; anas.hassan@ku.ac.ae
[4] Chemical Engineering Department, Universiti Teknologi PETRONAS, Seri Iskandar 32610, Malaysia; grace_20000207@utp.edu.my
* Correspondence: bennet_17006974@utp.edu.my (B.N.T.-O.); abdalla.ayoub@utp.edu.my (M.A.A.M.)

Abstract: Combinatory flooding techniques evolved over the years to mitigate various limitations associated with unitary flooding techniques and to enhance their performance as well. This study investigates the potential of a combination of 1-hexadecyl-3-methyl imidazolium bromide (C_{16}mimBr) and monoethanolamine (ETA) as an alkali–surfactant (AS) formulation for enhanced oil recovery. The study is conducted comparative to a conventional combination of cetyltrimethylammonium bromide (CTAB) and sodium metaborate ($NaBO_2$). The study confirmed that C_{16}mimBr and CTAB have similar aggregation behaviors and surface activities. The ETA–C_{16}mimBr system proved to be compatible with brine containing an appreciable concentration of divalent cations. Studies on interfacial properties showed that the ETA–C_{16}mimBr system exhibited an improved IFT reduction capability better than the $NaBO_2$–CTAB system, attaining an ultra-low IFT of 7.6×10^{-3} mN/m. The IFT reduction performance of the ETA–C_{16}mimBr system was improved in the presence of salt, attaining an ultra-low IFT of 2.3×10^{-3} mN/m. The system also maintained an ultra-low IFT even in high salinity conditions of 15 wt% NaCl concentration. Synergism was evident for the ETA–C_{16}mimBr system also in altering the carbonate rock surface, while the wetting power of CTAB was not improved by the addition of $NaBO_2$. Both the ETA–C_{16}mimBr and $NaBO_2$–CTAB systems proved to form stable emulsions even at elevated temperatures. This study, therefore, reveals that a combination of surface-active ionic liquid and organic alkali has excellent potential in enhancing the oil recovery in carbonate reservoirs at high salinity, high-temperature conditions in carbonate formations.

Keywords: surface-active ionic liquid; organic alkali; interfacial tension; wettability alteration; emulsification; alkali–surfactant flooding

Citation: Tackie-Otoo, B.N.; Ayoub Mohammed, M.A.; Zalghani, H.A.B.M.; Hassan, A.M.; Murungi, P.I.; Tabaaza, G.A. Interfacial Properties, Wettability Alteration and Emulsification Properties of an Organic Alkali–Surface Active Ionic Liquid System: Implications for Enhanced Oil Recovery. *Molecules* **2022**, *27*, 2265. https://doi.org/10.3390/molecules27072265

Academic Editor: Hany M. Abd El-Lateef

Received: 28 February 2022
Accepted: 21 March 2022
Published: 31 March 2022

1. Introduction

Chemical-Enhanced Oil Recovery (cEOR) methods have proven to be very efficient in mobilizing and extracting residual and remaining oils from matured reservoirs [1]. Primary and secondary oil recovery techniques leave a momentous volume of oil unrecovered, owing to trapping by capillary forces and unstable displacement fronts. The chemical flooding methods, such as the injection of alkali, surfactant, polymer, foam and low-salinity water, are used to recover trapped oil. Various hybrid techniques have been developed over the years to enhance the performances of individual techniques, as well as mitigate their limitations [2]. Alkali-augmented surfactant (AS), alkali-augmented polymer (AP), polymer-augmented surfactant (SP) and alkali–surfactant–polymer (ASP) flooding are

some of the hybrid techniques deployed for recovery [3]. In addition, nanoparticles are deployed to augment various flooding methods, like surfactant nanofluids, nanoparticle–nanoparticle–surfactant foam, polymeric nanofluids and smart nano-waterflooding [2,4–8].

Despite the promising nature of various chemical floodings and their hybrid techniques, the chemicals deployed have associated limitations that inhibit their worldwide application [9]. The inorganic alkalis conventionally deployed, like NaOH and Na_2CO_3, cause severe scaling problems, which impair reservoir permeability and lead to loss of production capacity [10–13]. Conventional surfactants have serious environmental concerns due to their low biodegradability and biocompatibility. Some of these surfactants precipitate in the presence of divalent cations and lose their functionality [14]. Several scholars have investigated and suggested alternatives in the literature [9]. They have proposed a switch to using organic alkalis as alternatives to inorganic alkalis. Monoethanolamine (ETA) has proven to be one of the most promising organic alkalis that have undergone extensive studies [10–13,15–17]. Renewable resource-based surfactants have also been proposed as alternatives to petrochemical-based surfactants due to their high biodegradability and biocompatibility [18–27]. Surface-active ionic liquids (SAILs) have also been proposed for surfactant application in harsh reservoir conditions (high-temperature and high-salinity reservoirs) [28,29].

Despite the economic significance of carbonate reservoirs (i.e., containing about 60–65% of the world's remaining oil-proven reserves [30–32]), their oil recovery poses a great challenge. Anionic surfactants are widely used in sandstone reservoirs due to their negative headgroup and, hence, adsorb less on the sand surface (surface charge of sand being negative). Cationic surfactants, on the other hand, have positive headgroups and are more suitable for residual oil recovery in carbonate rocks. Cetyltrimethylammonium bromide (CTAB), a cationic surfactant, has been proven by recent investigations to exhibit better wettability alteration capability on carbonate rock surfaces than anionic surfactants [33]. Furthermore, the widely deployed Na_2CO_3 in cEOR has limited applications in carbonate due to severe scaling problems in the presence of gypsum and anhydrite [34]. Sodium metaborate ($NaBO_2$) has been deployed as one of the alternative inorganic alkalis. It elevates pH without substantial permeability impairment. It also has high resistance to divalent cations and is a better alternative for carbonate reservoir application [35,36]. A combination of $NaBO_2$ and CTAB has been proven to exhibit synergistic performance in IFT reduction and wettability alteration, as well as the formation of stable emulsions.

Among the SAILs that have been investigated as alternatives to conventional surfactants, 1-hexadecyl-3-methylimidazolium bromide (C_{16}mimBr) has been studied comparatively to CTAB by Nandwani et al. [37]. C_{16}mimBr is considered a cationic surfactant, and this comparative study is justified by the similarity in its structure and aggregation behavior to that of CTAB. The structures of C_{16}mimBr and CTAB are shown in Figure 1. The two surfactants have the same hydrophobic chain lengths and counterions. C_{16}mimBr exhibited superior interfacial properties to CTAB in high-salinity conditions [37].

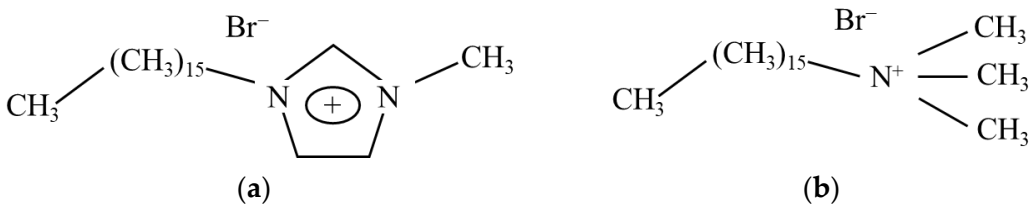

Figure 1. Chemical structures of (**a**) C_{16}mimBr and (**b**) CTAB.

Therefore, it has been proven in the literature that ETA and C_{16}mimBr have excellent potential as alternatives to inorganic alkalis and cationic surfactants in carbonate EOR applications. Nevertheless, a combination of these two alternative chemical agents that will yield better oil recovery through a synergistic performance has not be reported in the literature yet. Herein, an AS formulation comprising ETA and C_{16}mimBr is proposed.

This study focused on investigating the synergies that exist between ETA and C_{16}mimBr in enhancing oil recovery. First, the aggregation behavior of C_{16}mimBr is revisited and studied in comparison to CTAB. The proposed AS formulation's IFT reduction and wettability alteration capabilities are studied in comparison to a conventional AS formulation composed of $NaBO_2$ and CTAB. Finally, the interfacial properties of the formulation are confirmed through emulsification studies.

2. Materials and Methods

2.1. Materials

The details of the various materials used in this study are summarized in Table 1. The study utilized ETA and $NaBO_2$ as alkalis and C_{16}mimBr and CTAB as surfactants. Synthetic brine was prepared using nine salts. The brine composition and properties are presented in Table 2. A light crude oil from a Malaysian oil field was deployed as the oleic phase. Its composition and properties are also summarized in Table 2. The chemicals were used as received, and the deionized water was not purified further. The preparation and dilution of various chemical solutions and brine were done with deionized water.

Table 1. Details of the experimental materials.

Type	Materials	Purity *	Supplier
Surfactants	1-hexadecyl-3-methyl imidazolium bromide	AR, over 99%	Career Henan Chemical Co (Zhengzhou, China)
	Cetyltrimethylammonium bromide	AR, over 99%	Acros Organics (Semenyi, SGR, Malaysia)
Alkalis	Monoethanolamine	~99.5–100%	R and M chemicals (Subang Jaya, Malaysia)
	Sodium metaborate tetrahydrate	AR, 99.5%	Sigma-Aldrich (Petaling Jaya, Malaysia)
Salts	Strontium chloride hexahydrate, $SrCl_2{\cdot}6H_2O$	AR, 99%	Merck Chemicals (Petaling Jaya, Malaysia)
	Calcium chloride dihydrate, $CaCl_2{\cdot}2H_2O$	AR, 99.5%	R and M chemicals (Subang Jaya, Malaysia)
	Magnesium chloride hexahydrate, $MgCl_2{\cdot}6H_2O$	AR, 99.5%	R and M chemicals (Subang Jaya, Malaysia)
	Potassium chloride, KCl	AR, 99.5%	R and M chemicals (Subang Jaya, Malaysia)
	Sodium chloride, NaCl	AR, 99.5%	R and M chemicals (Subang Jaya, Malaysia)
	Sodium bicarbonate, $NaHCO_3$	AR, over 99%	R and M chemicals (Subang Jaya, Malaysia)
	Sodium sulfate, Na_2SO_4	AR, over 99%	R and M chemicals (Subang Jaya, Malaysia)
Oleic phase	Crude oil	-	Portray (M) SDN BHD (Petaling Jaya, Malaysia)

* AR is analytical reagent.

Table 2. Brine and crude oil compositions and properties.

Salt	Concentration (g/L)	Crude Oil Composition	% Weight
NaCl	23.9667	Saturates	55.6
KCl	0.7150	Aromatics	24.6
$MgCl_2{\cdot}6H_2O$	10.8322	Resins	16.3
$CaCl_2{\cdot}2H_2O$	1.5737	Asphaltenes	3.5
$SrCl_2{\cdot}6H_2O$	0.0201		
Na_2SO_4	4.0663		
$NaHCO_3$	0.2189		
Properties	Brine	Crude oil	
Density (g/mL) @ 25 °C	1.0229	0.8404	
Density (g/mL) @ 80 °C	0.98281	0.809	
Viscosity (mPa.s) @ 25 °C	1.041	13.6	
Viscosity (mPa.s) @ 80 °C	0.5334	6.3	
Salinity (mg/L)	41392.9		
Total acid number (mg KOH/g)		0.01	

An outcrop from a Malaysian carbonate formation was utilized for the wettability alteration studies. Thin slices of the rock sample with dimensions 20 × 20 × 3 mm were made and trimmed for contact angle measurements. The crushed and ground parts of the carbonate sample were then characterized using X-ray fluorescence (XRF) (model Bruker; S8 Tiger) and X-ray diffraction (XRD) (model X'Pert^3 Powder & Empyrean, PANanalytical). Fourier-transform infrared (FTIR) spectroscopy was then conducted with an FTIR spectrophotometer (Perkin Elmer Spectrum 2) within a wavenumber of 400–4000 cm^{-1}.

The XRF results presented in Table 3 confirm that the carbonate sample's predominant oxide is calcium oxide (96.7%), and 69.1% of the elemental composition is calcium. The carbonate sample is predominantly calcite, agreeing with the XRD results shown in Figure 2a. Figure 2b shows the FTIR spectrum for the carbonate sample, and various peaks corresponding to the vibration of the carbonate group could be observed. The in-plane and out-of-plane bending vibrations of the CO_3^{2-} group are shown by peaks at 712 cm^{-1} and 876 cm^{-1}, respectively. The asymmetric stretching of the CO_3^{2-} group is also shown by a peak at 1419 cm^{-1}. Then, an absorption peak at 1799 cm^{-1} corresponds to the symmetric stretching and in-plane bending vibration of the CO_3^{2-} group.

Table 3. Carbonate rock composition (XRF analysis).

Oxide	Concentration (%)	Elemental Composition	Concentration (%)
CaO	96.7	Ca	69.1
MgO	1.18	Mg	0.710
SiO_2	0.673	Si	0.315
P_2O_5	0.667	P	0.291
Al_2O_3	0.258	Fe	0.180
Fe_2O_3	0.257	Al	0.137
K_2O	0.0868	K	0.0720
SO_3	0.0789	Cl	0.0650
Cl	0.0650	S	0.0316
SrO	0.0299	Sr	0.0253

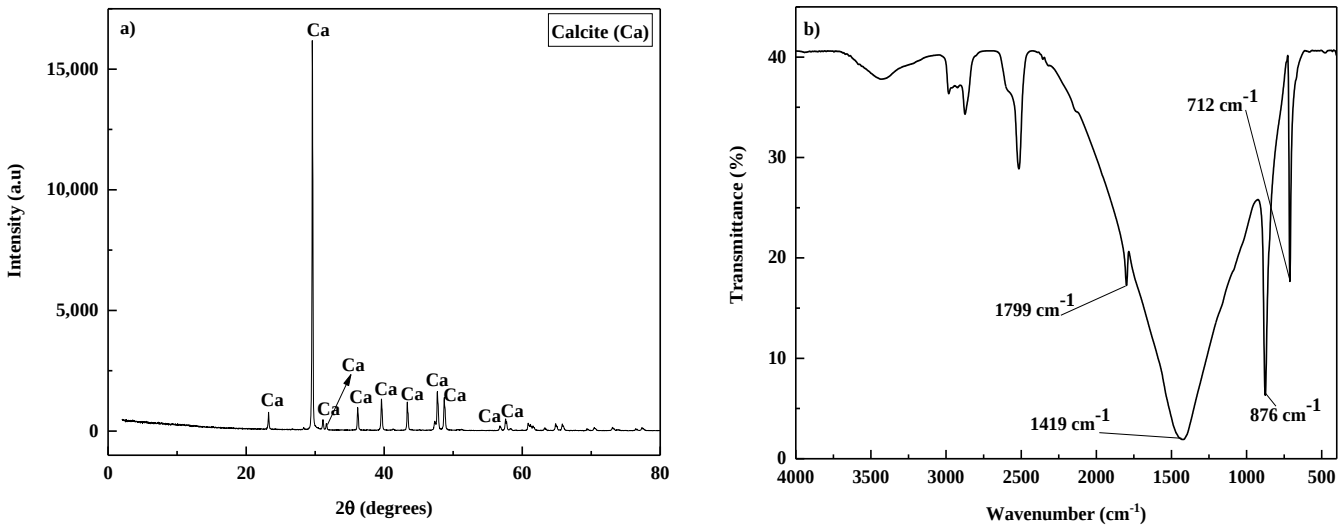

Figure 2. Characterization of a carbonate rock sample by (**a**) XRD and (**b**) FTIR.

2.2. Methods

The methods deployed in this study include surface tension and conductivity measurements to study the aggregation behaviors and surface activities of the surfactants. The aqueous stability test (i.e., compatibility with brine) was conducted to evaluate the tolerance of the various chemical agents and their combinations to hardness. The interfacial properties and wettability alteration of the surfactants, alkalis and their combination were investigated through IFT and contact angle measurements, respectively. Then, the final

step was an emulsification test to corroborate the interfacial properties. Figure 3 shows a flow chart of the experimental methods used in this study.

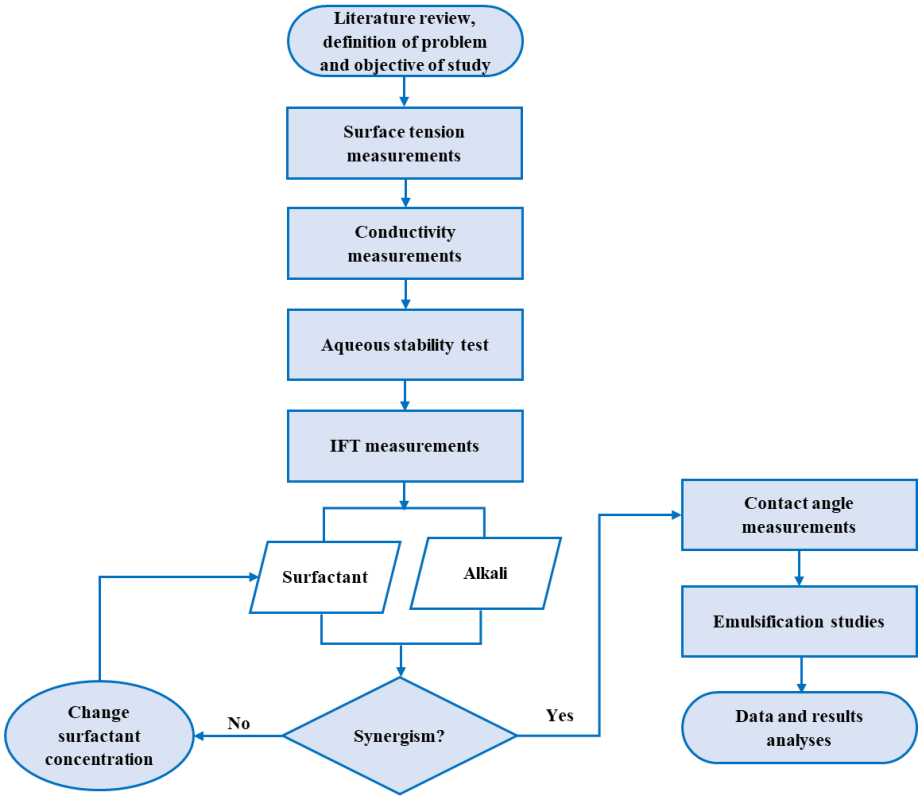

Figure 3. Flow chart of the experimental methods.

2.2.1. Surface Tension Measurements

The surface tension measurements of the aqueous solutions of the surfactants were made at different concentrations. The measurements were made using a Rame-Hart Model 260 goniometer (Ramé-hart instrument co., Succasunna, NJ, USA) at room temperature using the pendant drop method. The DROPimage Advance software was used in profile fitting the solution drop suspended from a needle in the air. Single measurements were made repeatedly with a standard deviation of 0.01–0.09 mN/m. Before the measurements, the equipment was calibrated with deionized water, and a value of 74.37 mN/m was found at room temperature.

2.2.2. Conductivity Measurements

Measurements of the electrical conductivities of the surfactant solutions were made at different concentrations with the aid of a Eutech Con 450 conductometer (Poly Scientific, Shah Alam, Malaysia) at room temperature. The surfactants' concentrations were varied by diluting stock solutions of the surfactants with ethanolamine solution. The solutions were stirred for about a minute and allowed to settle after every dilution before the conductivity measurements. The conductivities were recorded after allowing the reading to stabilize. Conductivity measurements at every concentration were repeated until the values were consistent. The estimated uncertainty was ±0.5 μS/m. Further analyses were made using the mean of three consistent values for each measurement.

2.2.3. Compatibility Test

The compatibility of the 1 wt% alkalis, 0.04 wt% surfactants and their combinations (1 wt% alkali and 0.04 wt% surfactant) with brine was tested. The focus was on evaluating the chemical agents' hardness tolerance and eliminating scale formation and surfactant pre-

cipitation during the flooding experiments. As observed from Table 2, the brine contained an appreciable number of divalent cations. The test was conducted for both the alternative and conventional chemical agents and their combination for comparative purposes. This test mixed aqueous solutions of alkalis, surfactants and AS combinations with the brine. The chemical formulation–brine mixture of a 50:50 volume ratio was used to simulate the contact of the injection and formation water within the reservoir. The mixtures were kept in glass tubes closed tightly, turned up and down a few times to ensure adequate mixing, then left for observation for a week at 80 °C and atmospheric pressure. The evaluation was solely visual, and any sign of precipitation indicated incompatibility.

2.2.4. Interfacial Tension Measurement

The IFT between crude oil and the various aqueous solution of the surfactants was measured using the spinning drop tensiometer (SVT 20, Data physics, Filderstadt, Germany) at room temperature. The measurement process involved the injection of the aqueous phase into a fast exchange capillary tube. The capillary tube was first set to rotate at a very low rotational speed (100–300 rpm); then, the crude oil droplet was injected. The low rotation during the crude oil droplet injection prevented the oil droplet from sticking to the walls of the capillary tube. The tube was then set to rotate at 5000 rpm, which caused the oil droplet to stretch. The elongated oil droplet was profile-fitted using SVT 20 software. The dynamic IFT was recorded at 20-s intervals until equilibrium was reached. The interfacial property in this study was based on the equilibrium IFT. To avoid interference from the former solution, the fast exchange capillary tube was cleaned with toluene, followed by acetone and deionized water, to remove the crude oil and surfactant residues. At ambient conditions, the IFT between crude oil and deionized water was 5.82 mN/m.

2.2.5. Contact Angle Measurements

Wettability alteration studies were done by measuring the contact angle of the surfactant aqueous solution on an oil-aged rock surface. The sessile drop method was applied in measuring the contact angles using the Rame-Hart Model 260 goniometer at ambient conditions. The rock slices described under the Materials section were utilized for the contact angle measurements. Toluene and methanol were used to first clean the slices, then dried. The oil wetness of the slices was induced by aging the slices in crude oil over a fortnight at 80 °C. Afterwards, n-heptane was used to rinse the oil-aged slices, then dried. The slices' initial wetting conditions were determined from the contact angle of the deionized water. The measurement process involved dropping the surfactant aqueous solution via a needle onto the slice. The solution then formed a sessile drop on the slice, which was analyzed by Young–Laplace fitting. The measurement was done for 10 min. The impact of cross-contamination from traces of the previous solution was mitigated by conducting each measurement on an unaffected part of the rock slice.

2.2.6. Emulsification Test

Emulsification is mostly the prevalent mechanism in surfactant oil recovery processes. Therefore, the emulsifying power of the surfactants–alkali combination and emulsion stability were also studied. The emulsification test involved homogenizing 3 wt% NaCl brine and crude oil using the surfactants at different concentrations as the emulsifying agent. The aqueous solution and crude oil were mixed at a 1:1 ratio in a 25-mL test tube. Homogenization was achieved using T18 digital ULTRA-TURRAX. The homogenized systems were left to equilibrate and observed over time while they disintegrated into their original component at 80 °C. The period of observation was one month, and the percentage reduction in the emulsion phase volume was used to analyze the stability of the emulsions formed. The percentage reduction in the emulsion phase volume is given by:

$$R_v = \frac{V_i - V_f}{V_i} \times 100 \quad (1)$$

where V_i is the original emulsion phase volume, and V_f is the emulsion phase volume after the period of settling.

3. Results and Discussion

3.1. Surface Activity and Aggregation Behavior of Surfactants

The surface activity of the surfactants was studied using the surface tension data. First, the critical micelle concentrations (CMC) of the surfactants were determined. A plot of the surface tension (γ) variation against the log of surfactant concentration (log C) is shown in Figure 4. The observed trend illustrates continuous surfactant adsorption onto the interface between air and water; after which, surface saturation occurs, then self-aggregation [38]. The breaking point on this semi-log plot corresponds to the CMC of the surfactant. The CMCs for the surfactants are given in Table 4. The surface tension method of determining CMC is very versatile, since data about the adsorbed layer at the air–water interface could also be derived [39]. The information on the adsorbed layer at the air–water interface is also presented in Table 4. It is apparent in Table 4 that C_{16}mimBr has a lower CMC than CTAB, despite the two having the same hydrophobic tail length. The difference in their CMC is therefore attributed to their headgroup. The planar imidazolium of C_{16}mimBr will ensure easier packing into the micelle than the tetrahedral trimethylammonium group of CTAB [40]. Additionally, Wintgens et al. [41] characterized the charge density on the cationic group of the surfactant using the headgroup charge per van der Waals volume. Trimethylammonium has a higher headgroup charge per volume (6.48) than 1-methylimidazolium (5.61). The higher headgroup charge per volume yields increased electrostatic repulsion among the headgroups and, hence, hinders the association of the micelles [41].

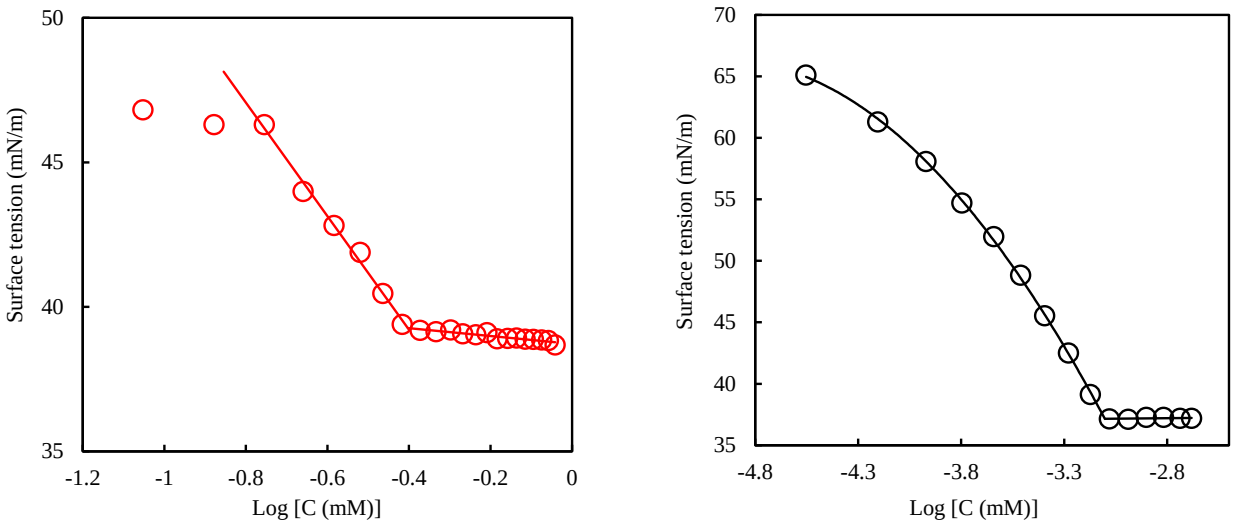

Figure 4. Surface tension versus logarithm of concentration for C_{16}mimBr (**left**) and CTAB (**right**) at 25 °C.

Table 4. Parameters obtained from the surface tension data at 25 °C.

Surfactant	CMC (mM)	Υ_{cmc} (mN/m)	pC_{20}	CMC/C_{20}	Π_{cmc} (mN/m)	Γ_m (μmol/m^2)	a^s_m (Å^2)
C_{16}mimBr	0.54	38.6	3.78	3.6	33.4	2.03	81.6
CTAB	0.84	37.01	3.67	3.93	34.94	2.78	59.73

Nevertheless, the difference in their CMC is not that significant; hence, a comparable dosage could be used in comparing their performances. CMC determination is routinely deployed to determine the optimum quantity of the surfactants in formulations. In the optimization of oil recovery, surfactant concentrations higher than the CMC are rather used to account for surfactant loss through adsorption on the rock surface.

The surface activity of the surfactants is discussed based on the efficiency and effectiveness in reducing the surface tension. The efficiency refers to the bulk phase concentration required to yield some amount of surface tension reduction. The effectiveness, however, is the maximum surface tension reduction that could be attained regardless of the bulk phase concentration [42]. The efficiency is evaluated using the pC_{20} calculated as:

$$pC_{20} = -\log C_{20} \quad (2)$$

where the C_{20} denotes the concentration of surfactant in the bulk phase needed to reduce a pure solvent's surface tension by 20 mN/m. In other words, the efficiency factor (pC_{20}) is the ability of a surfactant to yield a surface pressure of 52 mN/m at the lowest concentration possible [43]. It also depicts the adsorption efficiency [44]. The pC_{20} values from Table 4 show that C_{16}mimBr exhibited superior surface tension reduction efficiency compared to CTAB. Since the surface tension reduction efficiency is related to the bulk phase, the observed performance could be explained by the same phenomena that influenced the micellization.

The surface pressure at the CMC denoted by $\prod_{CMC}$ depicts the effectiveness of the surface tension reduction. The surface pressure is the difference in surface tension between a pure solvent and a surfactant solution at a particular concentration. The surface pressure at CMC is therefore shown by Equation (3) below. This parameter is used to measure the surface tension reduction effectiveness, because no profound reduction of surface tension after the CMC is attained.

$$\Pi_{CMC} = \gamma_0 - \gamma_{CMC} \quad (3)$$

The surface pressure values from Table 4 show that CTAB (Π_{cmc} = 33.4 mN/m) is more effective than C_{16}mimBr (Π_{cmc} = 34.94 mN/m), though the difference in their surface pressure values is marginal. The effectiveness of the surface tension reduction is dependent on the efficiency and effectiveness of the surfactant adsorption onto interfaces, as shown in Equation (4) [40]:

$$\Pi_{CMC} \approx 20 + 2.303nRT\Gamma_m \log\left(\frac{CMC}{C_{20}}\right) \quad (4)$$

In this equation, n represents the number of solute species with interfacial concentrations that vary with the bulk phase concentration variations, R is the universal gas constant (8.314 $JK^{-1}mol^{-1}$) and T is the absolute temperature in kelvin. The CMC/C_{20} ratio, which incorporates the efficiency of adsorption, depicts the spontaneity of micellization relative to adsorption [45]. The CMC/C_{20} ratio value increases because of the structural effect or microenvironmental factor that delays micellization or facilitates adsorption. Therefore, a decrease means the adsorption is hindered or micellization is facilitated [44]. The adsorption effectiveness of the surfactant is depicted by the surface excess concentration (Γ_m) and the minimum surface area per molecule at the interface at surface saturation ($a^s{}_m$). These parameters could be calculated with the Gibbs adsorption isotherm [40].

$$\Gamma_m = -\frac{1}{2.303nRT}\left(\frac{d\gamma}{d\log C}\right) \quad (5)$$

$$a_m^s = \frac{1}{N\Gamma_m} \quad (6)$$

The value of n is 2 for a dilute solution of 1:1 ionic surfactant [40]. N is Avogadro's number. From Equation (6), a parallel variation of the CMC/C_{20} ratio and Γ_m gives an easier explanation of the observed variation in $\prod_{CMC}$. Since C_{16}mimBr has a lower CMC/C_{20} ratio and Γ_m than CTAB, micellization is facilitated more in C_{16}mimBr, which leads to lesser surfactant molecules available at the interface to ensure more effective surfactant adsorption. This observation implies that a lower concentration of C_{16}mimBr is required to achieve the most effective surface tension reduction. A higher concentration,

however, is required for CTAB, but it can achieve a more effective surface tension reduction than C_{16}mimBr.

3.2. Conductivity and Thermodynamic Properties of Aggregation of Surfactants

The thermodynamic properties of aggregation for the surfactants were also studied using the conductivity data. The CMC is first determined from the conductivity versus surfactant concentration plot, as shown in Figure 5. Based on Williams' method, the breaking point on the conductivity variation with the surfactant concentration points to the CMC [46]. The CMC values from the conductivity method are also presented in Table 5. The CMC values showed similar variations as observed in the surface tension method, hence corroborating the CMCs determined. Nevertheless, for each surfactant, the CMC value determined by the conductivity method varies slightly from the surface tension. The methodical differences in CMC determination were explained by Mukerjee and Mysels [47]. The CMC, unlike a property-like a melting point, does not have a sharply defined point above which some properties are qualitatively different from below it. The methodical differences would have been nonexistent or minimal. However, all properties of a solution in the CMC region vary continuously and so do all their derivatives. There is, therefore, a relatively narrow region of concentration in which these changes are most marked. The CMC is therefore a narrow range of concentrations but not a single value.

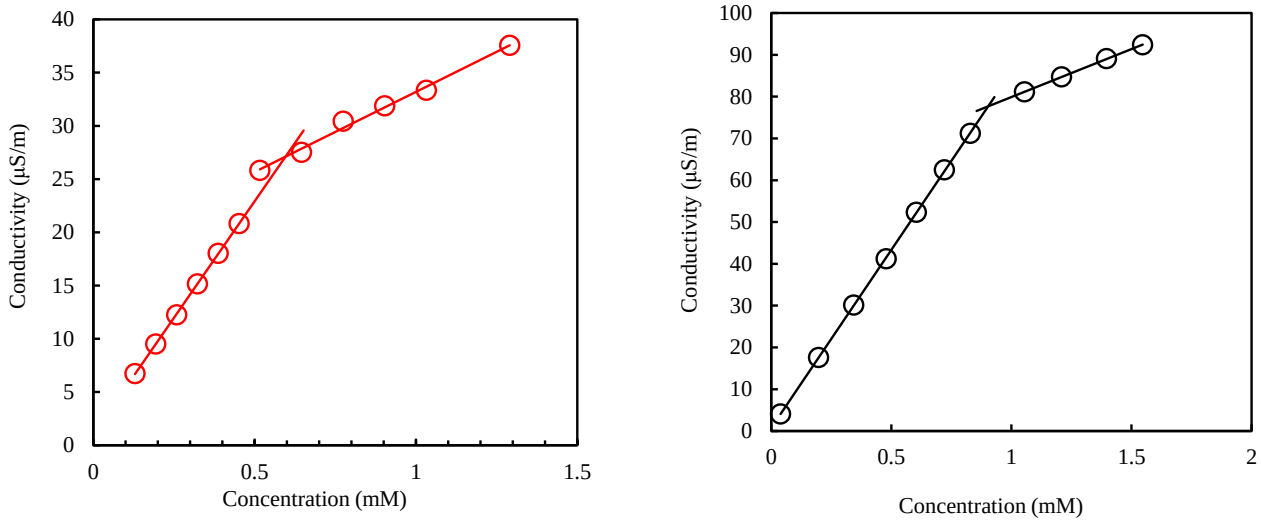

Figure 5. Conductivity versus concentration for C_{16}mimBr (**left**) and CTAB (**right**) at 25 °C.

Table 5. Thermodynamic parameters derived from conductivity data.

Surfactant	CMC (mM)	α	β	ΔG^{O}_{mic} (kJ/mol)	ΔG^{O}_{abs} (kJ/mol)
C_{16}mimBr	0.60	0.34	0.66	−46.97	−63.42
CTAB	0.85	0.27	0.73	−47.04	−59.62

From the CMC, the Gibbs free energy (ΔG^{O}_{mic}) of the micellization is computed using Equation (7) [48]:

$$\Delta G^{O}_{mic} = (1 + \beta)RT \ln X_{CMC} \quad (7)$$

R and T have their usual meaning in this equation. X_{CMC} represents the CMC in a mole fraction, and β depicts the degree of counterion binding of the micelle. β is derived from the degree of ionization (α). The degree of ionization is the ratio of the slope before CMC to the slope after CMC on the conductivity versus concentration plot. The relationship between the two parameters is given as $\beta = 1 - \alpha$ [49]. The process of surfactant adsorption onto

the interface could also be evaluated through the standard Gibbs free energy of adsorption (ΔG^{O}_{ads}). It is computed from ΔG^{O}_{mic} through Equation (8) [50]:

$$\Delta G^{O}_{ads} = \Delta G^{O}_{mic} - \frac{\Pi_{CMC}}{\Gamma_m} \quad (8)$$

As presented in Table 5, both ΔG^{O}_{mic} and ΔG^{O}_{ads} are negative, depicting that both the micellization and adsorption processes are spontaneous. The higher values of ΔG^{O}_{ads} also show that adsorption is more favored than micellization for both surfactants. In comparison to CTAB ($\Delta G^{O}_{mic} = -47.04$ KJmol^{-1} and $\Delta G^{O}_{ads} = -59.62$ KJmol^{-1}), the lower values of ΔG^{O}_{mic} for C_{16}mimBr showed that micellization is more spontaneous for CTAB, as the degree of binding is higher, owing to a smaller surface area per headgroup (a^{s}_{m}, as shown in Table 4). Nevertheless, the higher values of ΔG^{O}_{ads} for C_{16}mimBr show that its adsorption is more spontaneous.

3.3. Compatibility with Brine

A significant limitation in ASP application is scale formation by alkalis and surfactant precipitation due to the divalent cations' presence (mainly Mg^{2+} and Ca^{2+}). The effectiveness and efficiency of most conventional surfactants dwindle in the presence of divalent cations [9]. The precipitates formed reduce the production efficiency through pore blockage [14]. Insoluble scale formation is due to conventionally deployed inorganic alkalis with divalent cations and the reservoir. The insoluble scale formation leads to formation damage, production capacity reduction, lifting system damage and reduction in the average pump-checking period [51–53]. Therefore, it is vital to consider the hardness tolerance of surfactants in their EOR applications [54]. The rule of thumb is to maintain the concentrations of divalent ions below 10 ppm for efficient alkali application [11]. Therefore, massive pre-flush and other costly measures, such as water treatment by ion exchange or other techniques for softening brine, are required to ensure efficient oil recovery [11,55]. The hardness tolerance of ionic surfactants is also improved by adding nonionic surfactant or alcohol to their formulations [54].

The compatibility of alkalis, surfactants and AS formulations with brine is shown in Figure 6. The ETA was incompatible with brine, while $NaBO_2$ formed a stable and clear solution with brine. With higher divalent cation concentrations, the hardness tolerance of ETA is exceeded. The ethanolamines, diethanolamine and triethanolamine are more tolerant to hardness than ETA [56]; nevertheless, ETA has been proven to have a better synergistic effect with the surfactant in IFT reduction [12]. Therefore, ETA was the choice for this study among the ethanolamines. $NaBO_2$, on the other hand, is known to sequester divalent ions [57,58]. C_{16}mimBr and CTAB were not expected to form a precipitate with brine, since they are cationic surfactants [14]. Both the combination of ETA with C_{16}mimBr and $NaBO_2$ with CTAB formed a clear solution with brine. Therefore, no precipitations and formation damage are expected in their flooding process.

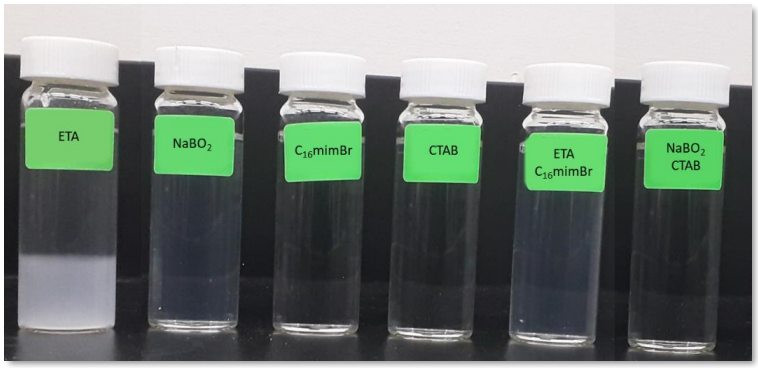

Figure 6. Compatibility of the chemical solutions with brine.

3.4. Interfacial Properties

IFT reduction is known to be a predominant mechanism in the application of the surfactant and alkali for enhancing oil recovery. The interfacial properties of these chemical agents are therefore vital in developing an optimum formulation for improving oil recovery. Herein, the performance of the ETA–C_{16}mimBr combination in reducing IFT is evaluated in comparison to a $NaBO_2$–CTAB combination, both in a deionized water and brine solution. The effect of temperature is evaluated as well. The IFT reduction capability of C_{16}mimBr is first compared to CTAB, as presented in Figure 7. C_{16}mimBr had a similar IFT reduction capability as CTAB, with a minimum IFT (IFT_{min}) of 0.055 mN/m (at 0.03 wt% C_{16}mimBr concentration), and CTAB had an IFT_{min} of 0.053 mN/m (at 0.04 wt% CTAB concentration). This observation confirms their surface activity, as explained in Section 3.1. C_{16}mimBr attains IFT_{min} at a lower concentration, owing to the facilitated micellization process. Due to the delayed micellization in CTAB, there more surfactant molecules available at the oil–water interface to reduce IFT further. The predominant surfactant feature that enhances the IFT reduction capability is the alkyl chain length [40]. The two cationic surfactants have the same alkyl chain length, which masks the difference in the interfacial properties caused by the differences in their headgroups, hence the similarities in their interfacial properties.

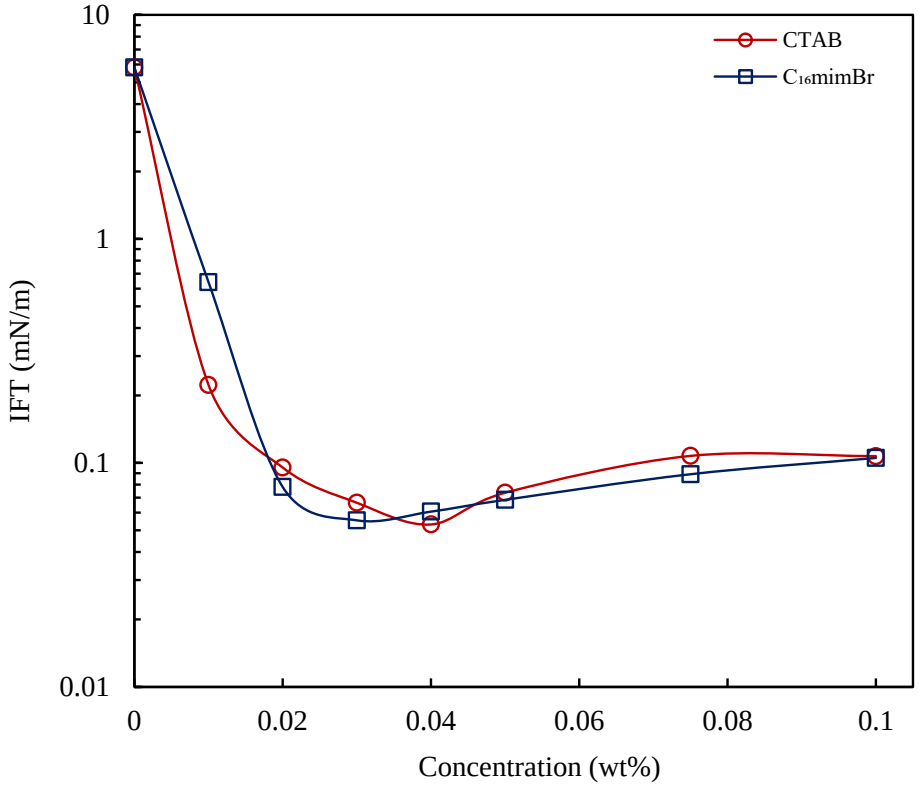

Figure 7. Aqueous–crude oil IFT variation with the surfactant concentration at 25 °C.

3.4.1. Effect of Alkali

The combination of alkali and surfactant is known to yield synergistic perfor mances [3,34,59,60]. Based on the IFT reduction studies of the surfactants, concentrations of 0.02 wt% and 0.01 wt% were chosen. The two cationic surfactants achieved IFT_{min} at different concentrations; therefore, 0.02 wt% is chosen as a common concentration to investigate the effect of alkalis. The IFT reduction of alkalis at various surfactant concentrations is presented in Figure 8. At a 0.02 wt% surfactant concentration, a synergistic effect was observed for both surfactants. C_{16}mimBr at 0.02 wt% reached an IFT_{min} of 7.6×10^{-3} mN/m at a 0.3 wt% ETA concentration. Comparing this value to the IFT_{min} attained by C_{16}mimBr without alkali (i.e., IFT_{min} of 0.055 mN/m), there is evidence of synergism in the combination of C_{16}mimBr and ETA. An ultra-low IFT is achieved at a

lower surfactant concentration upon the addition of alkali. The combination of $NaBO_2$ and CTAB also yielded an IFT_{min} of 0.0318 mN/m (at a lower surfactant concentration), which is better than the IFT_{min} attained by CTAB without alkali. This observation agrees with the report of Kumar and Mandal [61] on the IFT reduction capability of the CTAB–$NaBO_2$ combination. The subsequent reduction in surfactant concentration to 0.01 wt% also yielded a synergistic effect, as shown in Figure 8. Nevertheless, the IFT reduction at a 0.02 wt% surfactant concentration was better.

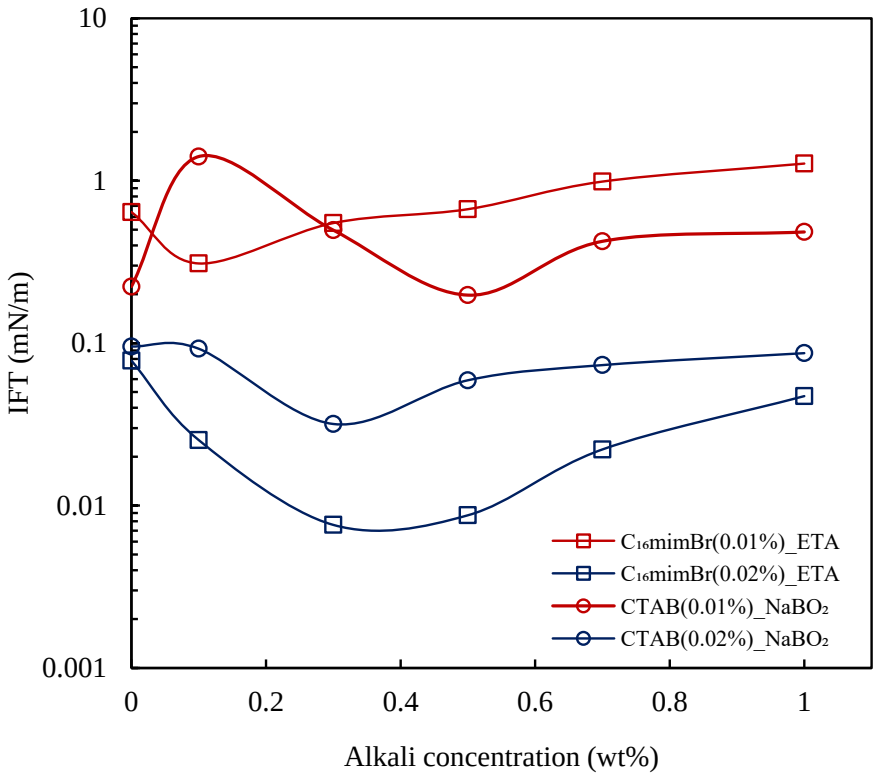

Figure 8. Effect of alkali on the oil–aqueous IFT.

3.4.2. Comparison of Synergism

The IFT reduction capability of the ETA–C_{16}mimBr combination is compared to the $NaBO_2$–CTAB combination to explore its performance. Firstly, the alkali performance in IFT reduction is discussed and presented in Figure 9. It is well-established in the literature that inorganic alkalis ($NaBO_2$) reduce IFT via the formation of an in situ surfactant through the deprotonation of acids. This phenomenon is caused by the ability of the inorganic alkalis to form carbonic acid that removes free H^+ ions from the solution [3]. In this study, the ETA did not reduce the IFT as much as reported in the literature [16]. As explained by Bai et al. [16], ETA renders the aqueous solution basic through the amine group in its structure, which generates an in situ surfactant by reacting with the saponifiable component of crude oil. They also explained that ETA has an amphiphilic structure owing to its alkyl and hydroxyl group and, hence, could act as a surfactant. Both alkalis yielded a low IFT reduction performance due to the crude oil's low acid content (TAN = 0.01 mg KOH/g) though the $NaBO_2$ performed better [62]. This observation proves that the amphiphilic nature of ETA does not guarantee the ability to reduce IFT. Therefore, ETA could not be considered as a surfactant capable of reducing IFT on its own. A longer alkyl chain length is a prerequisite for effective IFT reduction by an amphiphilic substance [40].

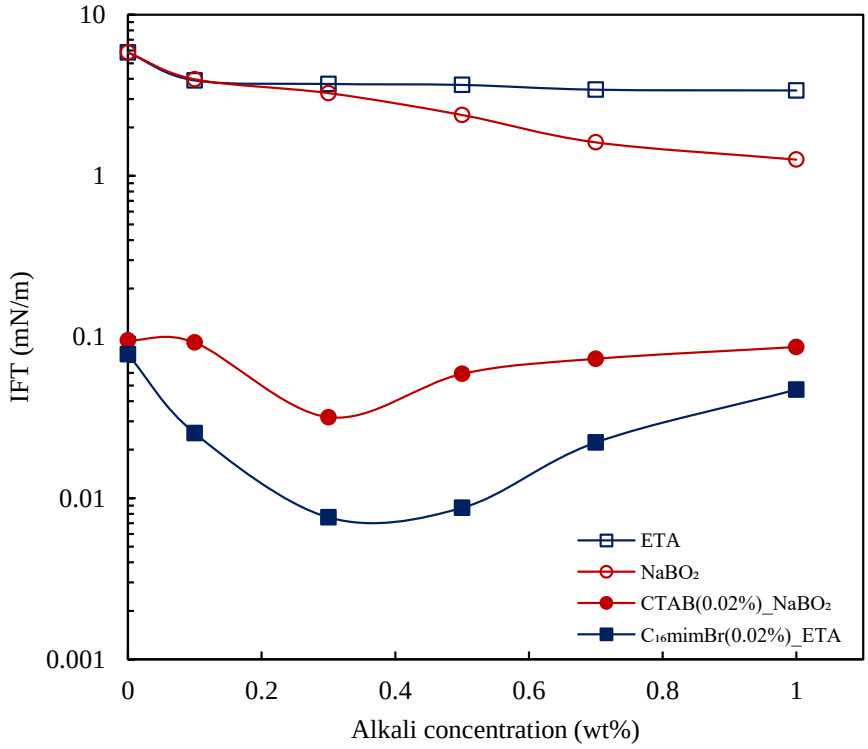

Figure 9. Aqueous–crude oil IFT variation with alkali concentration for chemical solutions at 25 °C.

Nevertheless, the ETA–C_{16}mimBr system reduced IFT better than the $NaBO_2$–CTAB system showing a better synergism, as seen in Figure 9. The performance could be attributed to in situ soap generation. Inorganic alkalis ($NaBO_2$) generate cationic petroleum carboxylate, but the nonionic alkanolamide soap generated by organic alkalis (ETA) gives a better synergy with the surfactants [22,63]. Furthermore, ETA and the generated in situ soap form a mixed surfactant system with the surfactant, which ensures tighter and better interfacial packing leading to the improved effectiveness of IFT reduction [12,16]. In the $NaBO_2$–CTAB system, the low acidic crude oil component limits the in situ soap generation. Therefore, there would be insufficient saponin to form the mixed surfactant system with the CTAB and, hence, less synergistic performance.

3.4.3. Effect of Salinity

The salinity has a significant impact on the interfacial properties. Generally, salt yields a synergistic effect with surfactants in reducing the IFT [22,23]. The effect of salt concentrations on IFT reduction by both AS formulations is shown in Figure 10. Both formulations improved in their IFT reduction capabilities in the presence of salt. The improvement in IFT reduction is attributed to a reduction in electrical repulsion due to the presence of opposite ions of the salt. The salt ions may also present competition with cations and anions of the surfactants in attracting water molecules, therefore reducing the solubility of surfactants [64]. The increase in salt concentration first resulted in further reduction in IFT to ultra-low levels at an optimum salinity of 6 wt% NaCl. The ETA–C_{16}mimBr system attained an IFT_{min} of 2.3×10^{-3} mN/m, while the $NaBO_2$–CTAB system attained an IFT_{min} of 4.95×10^{-3} mN/m. Further, an increase in salt concentration beyond the optimal salinity resulted in increasing the IFT. This observation could be attributed to the desorption of surfactant molecules at a high salinity and their subsequent dissolution into the oil phase [65]. Nevertheless, the IFT of the ETA–C_{16}mimBr system remained ultra-low even at very high salinity (i.e., 15 wt% NaCl concentration). This observation shows that the ETA–C_{16}mimBr system would be a good candidate for application in high salinity conditions.

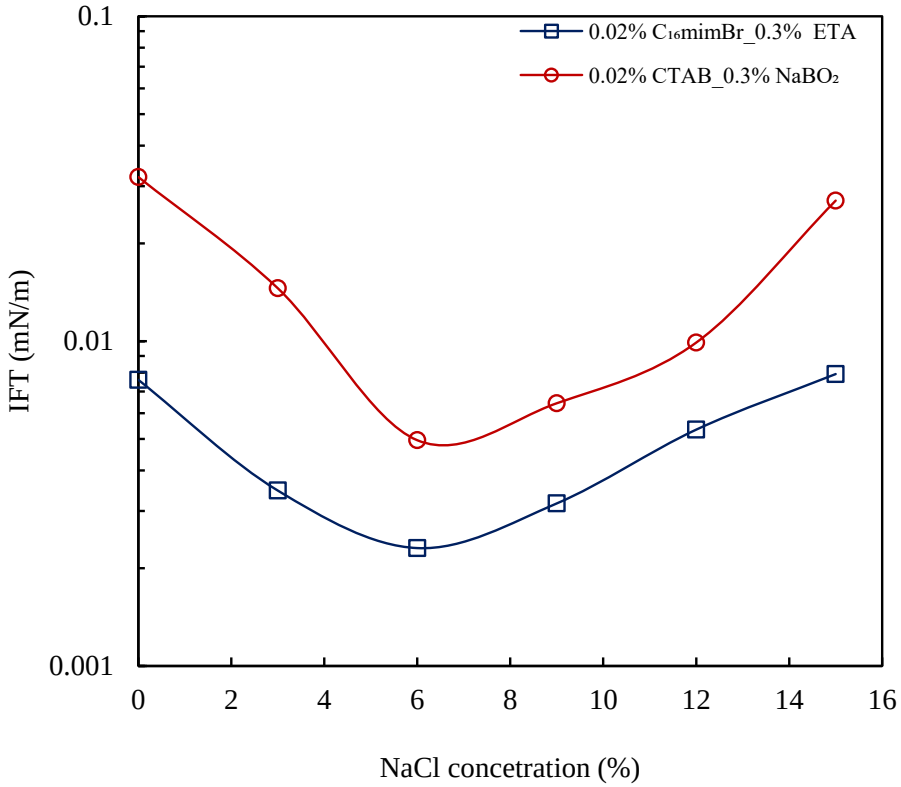

Figure 10. Salinity effect on IFT reduction by AS formulations at 25 °C.

3.4.4. Effect of Temperature

The IFT reduction capabilities of the surfactants are best explained based on their effectiveness and efficiency of adsorption onto the oil–water interface. Generally, for ionic surfactants, a temperature increase causes a decrease in adsorption effectiveness and efficiency. This observation could be ascribed to the improved solubility of surfactant molecules at elevated temperatures, limiting the concentration of surfactant molecules at the oil–water interface [40]. Nevertheless, the literature has reported contradicting findings on the IFT response to temperature [66]. From the observation made in this study during the IFT measurement process confirmed by the study of Okasha [67], the observed temperature effect on IFT is predominantly due to the type of crude oil. IFT between a dead oil and brine system reduces with the temperature increase, while IFT between a live oil and brine system increases [67]. As observed in this study, with increasing the temperature, dissolved gas in crude oil expands, resulting in an increase in density difference and the radius of the crude oil droplet. Referring to the relation for determining the IFT, as shown in Equation (9) [23], the IFT is expected to increase. The IFT variations with the temperatures for both AS formulations are shown in Figure 11. Both formulations exhibited increased IFT with the temperature increase. The live oil effect overshadowed the performance of the formulations at high temperatures. Therefore, the IFT reduction performance of both formulations at elevated temperatures is further investigated through emulsification studies, as low IFT is required to generate stable emulsions.

$$\sigma = \frac{\omega^2 R^3 \Delta\rho}{4} \quad (9)$$

where ω is the angular velocity, R is the crude oil droplet radius and $\Delta\rho$ is the difference in density between an aqueous solution of surfactant and crude oil.

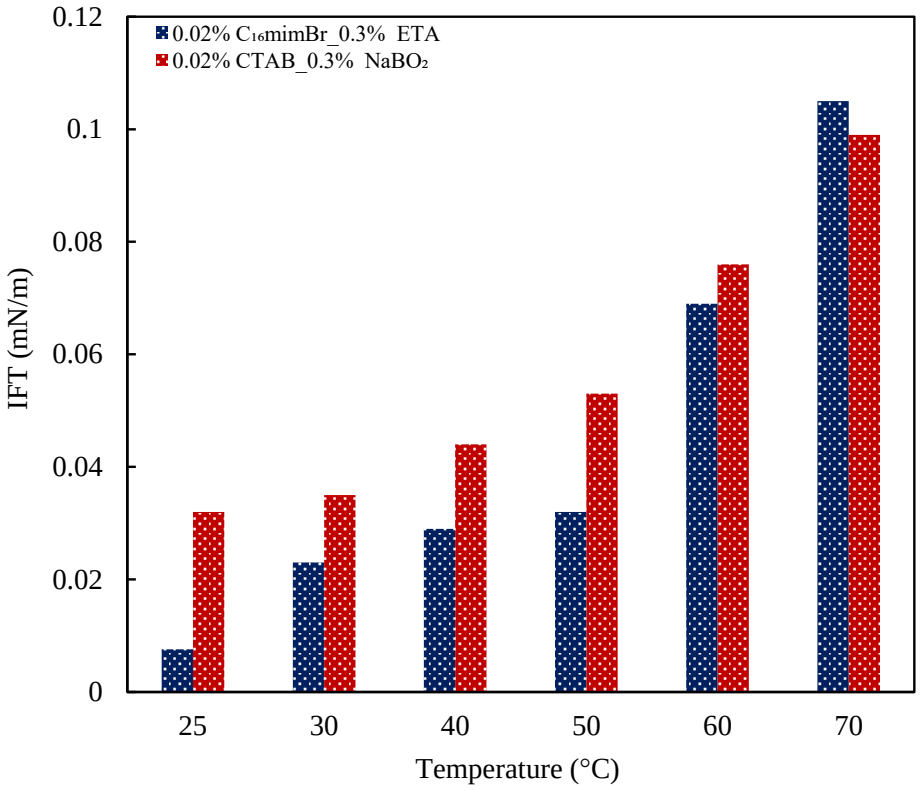

Figure 11. Effect of temperature on IFT reduction by AS formulations.

3.5. Wettability Alteration Characteristics

A favorable displacement is achieved in the multiphase flow of oil and water in the reservoir when the displacing fluid preferentially wets the rock surface. However, not all reservoirs are wet with water. Due to the prolonged oil storage within reservoirs, most oil reservoirs are either intermediately wet or wet with oil [68,69]. The wetting process involves surfaces and interfaces. Therefore, the ability to modify the wetting power of water or an aqueous solution is a surface property exhibited by all surfactants, yet to a greatly varied extent [40]. Surfactant and/or alkali application in EOR also yields favorable oil displacement by ensuring the aqueous phase preferentially wets the rock surface.

3.5.1. Wettability Alteration by Surfactants

The dynamic contact angle at various concentrations for C_{16}mimBr and CTAB is shown in Figure 12. From both figures, it is observed that the contact angle of water varies from 116° to 97° in 10 min. This means the carbonate surface is wet with oil. From Figure 12a, it is observed that the contact angle decreases significantly with the increasing C_{16}mimBr concentration. Beyond a 0.01 wt% concentration, the decrease in the contact angle becomes marginal. However, for the CTAB solutions (Figure 12b), the contact angle reduced further with the increasing CTAB concentration. Comparing the initial and final contact angles at various concentrations for C_{16}mimBr and CTAB, it is apparent that the CTAB solutions exhibited better wettability alteration capabilities than C_{16}mimBr. The surface activity study showed that CTAB has a higher Γ_m, which means more surfactant molecules are available at the solid–liquid interface to alter the rock surface wettability. Both surfactants have positive headgroups, and with the positive charge surface of carbonate, the observed wettability alteration is mainly attributed to the ion pair mechanism. The negative components of crude oil, predominantly fatty acids and carboxylate anions, adsorb onto the positive surface of carbonate and render it wet with oil [70]. The positive headgroups of C_{16}mimBr and CTAB form ion pairs with the negative crude oil component adsorbed on the carbonate surface and detach them, leaving the rock surface wet with water [33].

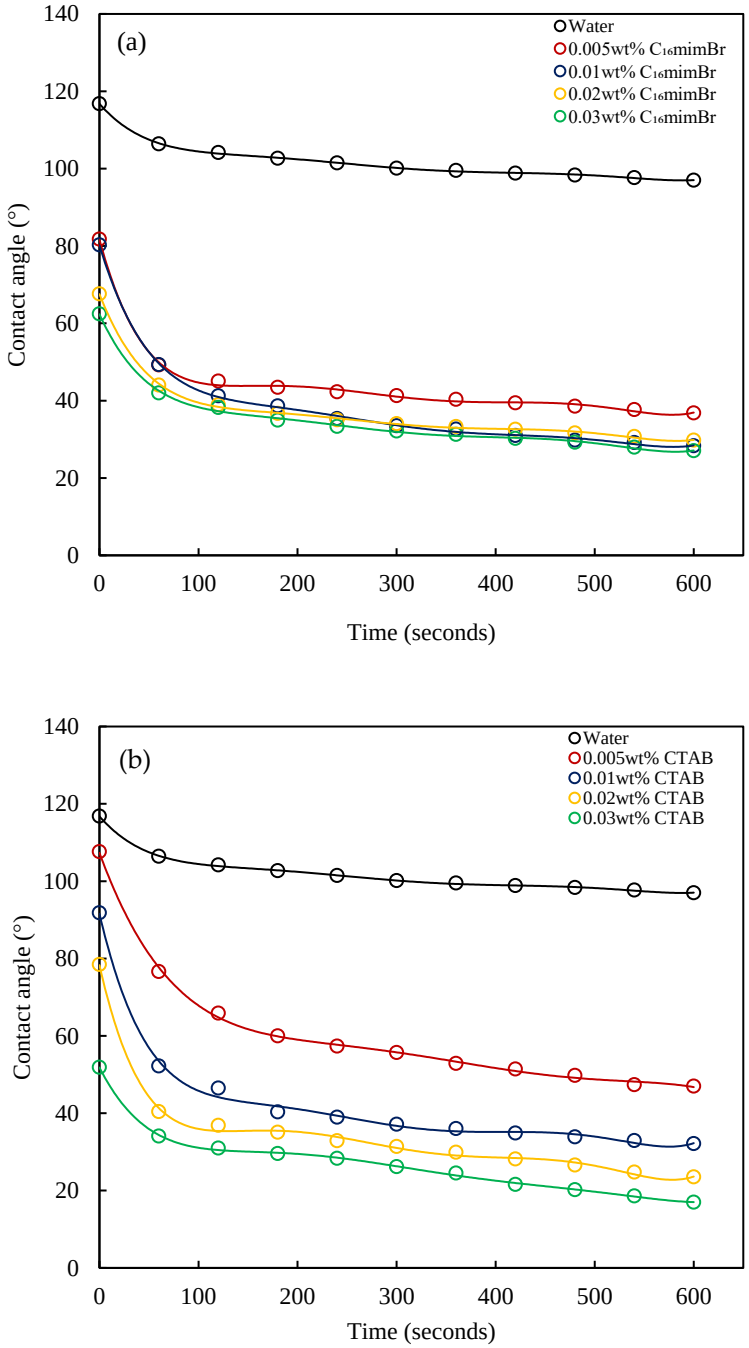

Figure 12. The dynamic contact angle of (**a**) C_{16}mimBr and (**b**) CTAB on a carbonate surface.

3.5.2. Wettability Alteration by Alkalis

The mechanisms in the application of alkali to enhance oil recovery are displacement through low IFT, breaking of a rigid film and wettability reversal [71]. However, wettability reversal becomes the preponderant mechanism in reservoirs with light crude oil [72]. In alkali flooding, the properties of the crude oil determine the predominant mechanism. The mechanisms, therefore, are associated with the general classes of compounds, like asphaltenes, acids, etc., in the crude oil [72]. This study used a crude oil with a low acidic content; hence, wettability reversal by an alkali would be an essential mechanism in recovering this crude oil type. Nevertheless, alkali application in carbonate reservoirs is limited due to the presence of anhydrite and gypsum, which cause precipitation problems. Carbonate reservoirs also contain brine with higher divalent cation concentrations [3].

Therefore, the wettability reversal by inorganic alkalis like NaOH and Na_2CO_3 in carbonate reservoirs are limited in the literature. Among the alternative alkalis to alleviate the precipitation problems are $NaBO_2$ and organic alkalis [9]. Nevertheless, their wettability alteration capabilities in carbonate formations are not reported in the literature. Herein, the wettability reversal by $NaBO_2$ and ETA is explored through contact angle measurements. The dynamic contact angles at different concentrations of ETA and $NaBO_2$ are presented in Figure 13. As shown above, the contact angle variations with time for water are from 116° to 97°, indicative of a wet oil condition. From Figure 13a, it could be observed that, except for the anomaly at a 0.7 wt% ETA concentration, further reduction in the contact angle is observed with the increasing ETA concentration. At a 1.0 wt% ETA concentration, the dynamic contact angle varied from 102° to 65°, depicting the ETA capability in altering the carbonate surface wettability. On the other hand, $NaBO_2$ exhibited the most effective wettability alteration capability at a 0.1 wt% concentration (dynamic contact angle varied from 90° to 54°). A further increase in the concentration resulted in reduced effectiveness in the contact angle reduction.

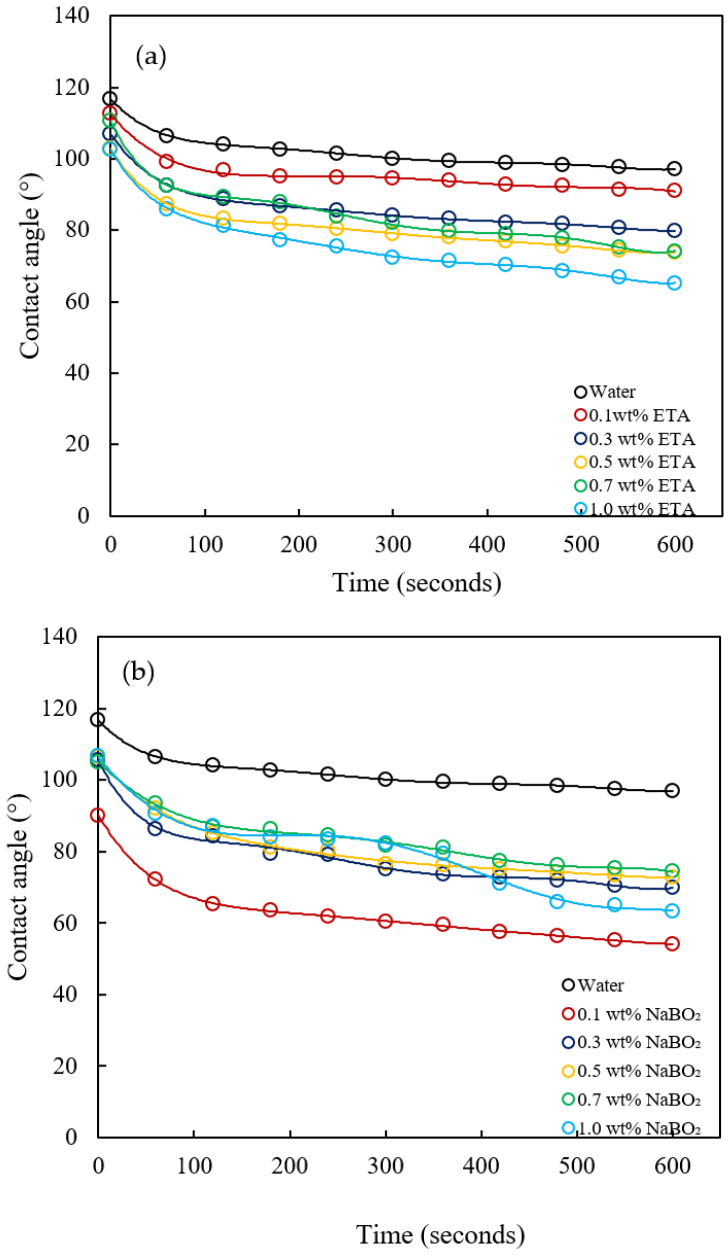

Figure 13. The dynamic contact angle of (**a**) ETA and (**b**) $NaBO_2$ on a carbonate surface.

Comparatively, $NaBO_2$ exhibited better wettability alterations than ETA, though the difference in their performances was marginal, as demonstrated in Figure 14. The figure shows a comparison of the initial and final contact angles at different alkali concentrations. Both alkalis render the surface of the carbonate rock moderately water wet. Various wettability reversal mechanisms have been proposed for inorganic alkalis; yet, the well-established ones are ion exchange and alkali interactions with rock [3]. The wettability reversal could also occur through alterations of the oil–water or liquid–solid IFT [72]. ETA, being a weak alkali, would have a weak interaction with the rock; therefore, wettability reversal is not as effective as in the case of inorganic alkalis [73]. This interaction yields hydrogen bonding between its hydroxyl group and the rock minerals, replacing the polar compounds adsorbed on the rock surface [17].

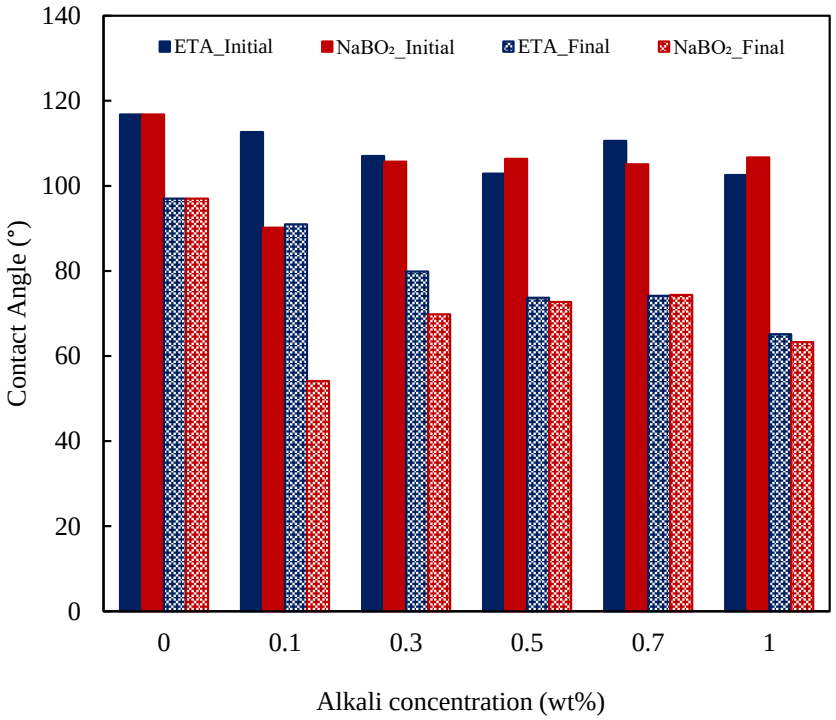

Figure 14. Initial and final contact angle variations with the alkali concentrations for ETA and $NaBO_2$.

3.5.3. Synergism in Wettability Alteration

The addition of alkalis also augments the wettability alteration performances of the surfactants [74]. The synergistic performance of the alkali–surfactant combination in wettability alteration is evident both in the contact angle reduction [61,75] and spontaneous imbibition [76]. The AS systems formulated to explore the synergism in the wettability alteration are composed of 1.0 wt% alkali and 0.01 wt% surfactant. The dynamic contact angle of the two AS formulations compared with their chemical agents is shown in Figure 15. The wettability alteration by the ETA–C_{16}mimBr system showed evidence of synergism. On the other hand, the addition of $NaBO_2$ to CTAB yielded a marginal improvement in the performance of CTAB. The observed synergism is attributed to the combined effect of different mechanisms of wettability alterations by surfactants and alkalis [73].

Alkalis react with an acidic component of crude oil to generate soap in situ, as explained under interfacial properties. A mixed surfactant system forms between the in situ soap and the surfactant with enhanced wetting power [40]. Nevertheless, the low acidic content of the crude oil will result in the generation of insufficient soap; therefore, this phenomenon is likely to be less effective. This explains the marginal performance between CTAB and the $NaBO_2$–CTAB system. On the other hand, ETA's amphiphilic nature means it could form a mixed surfactant system with C_{16}mimBr. The nonionic ETA could increase the C_{16}mimBr mobility, resulting in rapid molecular diffusion to the

wetting front [77]. This phenomenon improves the wetting power of C_{16}mimBr, hence the observed improved performance in the ETA–C_{16}mimBr system. Another explanation could be the improved solubilization of C_{16}mimBr by ETA, which enhances its wetting properties [78]. The ETA–C_{16}mimBr system, therefore, exhibited better wetting power than the $NaBO_2$–CTAB system.

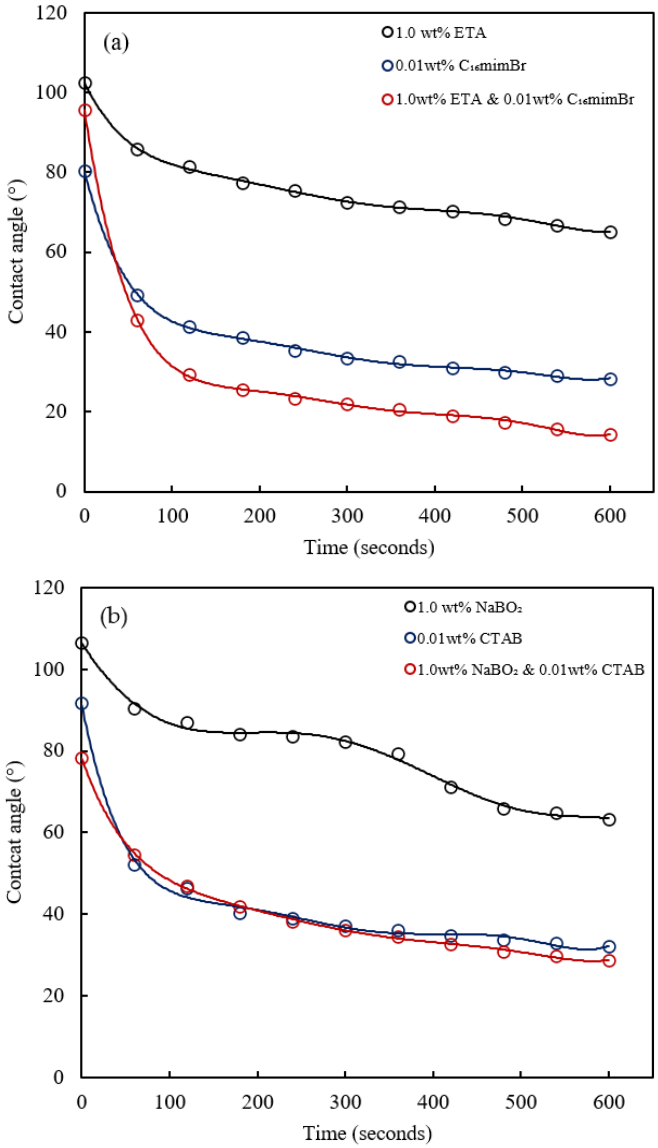

Figure 15. The dynamic contact angle of (**a**) ETA, C_{16}mimBr and the ETA–C_{16}mimBr system and (**b**) $NaBO_2$, CTAB and the $NaBO_2$–CTAB system on a carbonate surface.

3.6. Emulsification Studies

The emulsification mechanism causes oil to be entrained and produced in water. The oil droplets could also merge and block pores to improve the sweep efficiency by the emulsification and entrapment mechanism [3,79]. Surfactants facilitate the dispersion and emulsification of particles and droplets due to their amphiphilic nature. Nevertheless, emulsions generally demonstrate kinetic stability, since there is the tendency for the system to disintegrate and reduce the interfacial area and energy [80]. Emulsification and the stabilization of emulsions require low IFT between the immiscible fluids and the application of an adequate shear to promote homogenization [81].

To corroborate the observed IFT reduction capability of the various AS formulations and the effect of salinity and elevated temperature on their interfacial properties, emulsion

stability studies are conducted at a 3 wt% NaCl concentration and 80 °C temperature. Aqueous solutions of surfactants at 0.02 wt% and alkali at concentrations 0 to 1 wt% and electrolytes were mixed with the crude oil and homogenized at 5000 rpm for 10 min. The emulsion stability is inferred from the phase volume ratio variations observed for one month, as presented in Figure 16.

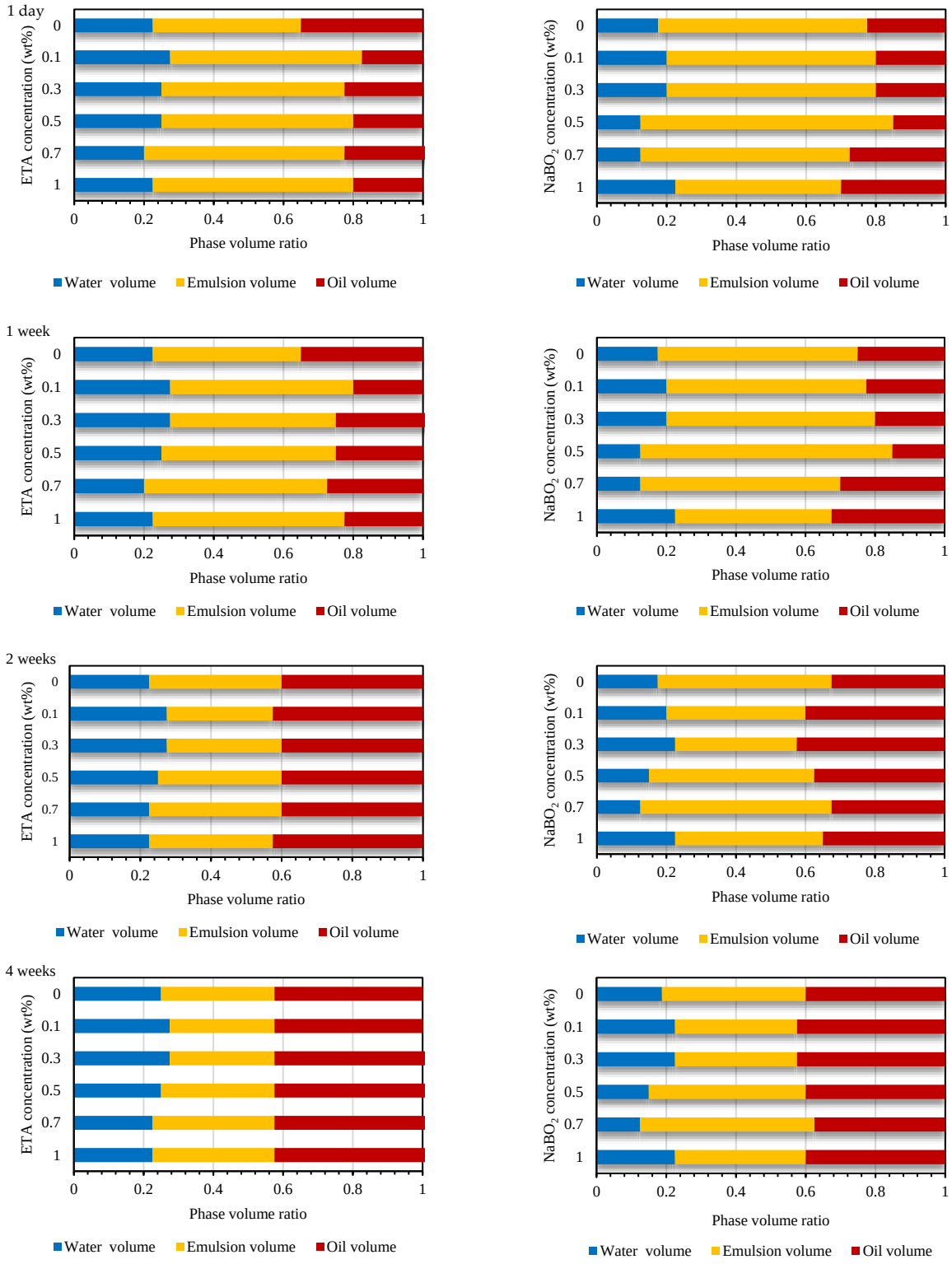

Figure 16. Emulsion stability of the ETA–C_{16}mimBr (**left**) and $NaBO_2$–CTAB (**right**) systems at various alkali concentrations at 80 °C.

With the addition of a surfactant and/or alkali, the emulsification mechanism could be based on the surface tension theory [40]. The reduction of IFT by the surfactants and alkali reduced the amount of mechanical work required to break the inner phase into dispersed particles. Both C_{16}mimBr and CTAB are known to form emulsions with smaller droplet sizes and narrow droplet size distributions yielding stable emulsions [37,61]. The percentage reduction in the emulsion phase volume over one month for C_{16}mimBr was ~24%, while that of CTAB was ~31%. Nevertheless, the $NaBO_2$–CTAB system formed more stable emulsions with a percentage reduction in the emulsion phase volume in the range of ~17–42%, while the ETA–C_{16}mimBr system also formed a stable emulsion with an emulsion phase volume reduction in one month of ~39–45%. For both systems, it was observed that emulsion stability decreased upon the addition of alkali, then improved with the increasing alkali concentration.

The emulsions formed are oil in water (o/w)-type emulsions. The emulsion type formed is due to the hydrophile–lipophile balance (HLB) of the surfactants [82]. The disintegration of the emulsion phase also resulted in an increase the oil phase, as seen in Figure 16. This observation means oil is the dispersed phase. With the formation of o/w emulsions, the stability of the emulsions formed is due to the existence of an electrical or steric barrier to coalesce on the dispersed droplets [40]. The source of the charge on the dispersed droplets is the adsorbed layer of the surfactant with its hydrophilic head oriented toward the aqueous phase. Therefore, the charge on the oil droplets that yields the repulsive force to keep them dispersed is that of the amphipathic ion of C_{16}mimBr and CTAB.

Another factor that reduces the rate of coalescence of the oil droplets is the mechanical strength of the interfacial film surrounding the oil droplets. The stronger the film, the less chance of coalescence upon the collision of oil droplets. The strength of the interfacial film is dependent on the tighter packing of surfactant molecules on the oil/water interface. The packing is tighter with the increasing alkyl chain length of the surfactants, and that explains why both systems formed stable emulsions. $NaBO_2$ as an inorganic alkali would act as a salt and reduce the electrostatic repulsion among the CTAB headgroups, yielding tighter packing and more stable emulsions. For the ETA–C_{16}mimBr system, a mixed surfactant system is formed between ETA and C_{16}mimBr, which also yields tighter packing and stable emulsions, but the emulsion stability study proved that the former phenomenon is more effective. Therefore, based on the emulsification studies, it could be concluded that both AS formulations are stable at elevated temperatures.

4. Conclusions

A combination of C_{16}mimBr and ETA was investigated for its possible application in alkali–surfactant flooding. The two chemical agents have been proposed in previous studies as alternatives to conventional surfactants and alkalis, respectively. It is believed that their application could mitigate the effect of the limitations associated with their conventional counterparts. Thus, this proposed AS formulation was studied in comparison to a conventional AS formulation made of CTAB and $NaBO_2$. The following conclusions could be deduced from this study:

The study confirmed that C_{16}mimBr and CTAB have similar aggregation behaviors and surface activities.

Though ETA exhibited an incompatibility with brine, its combination with C_{16}mimBr proved to eliminate the issue of scaling and surfactant precipitation. The conventional chemicals deployed in this study were also compatible with brine, as reported in the literature.

The addition of the alkalis to the surfactants exhibited a synergistic performance in IFT reduction for both AS formulations. The ETA–C_{16}mimBr system proved to be better than the $NaBO_2$–CTAB system in IFT reduction, yielding an ultra-low IFT of 7.6×10^{-3} mN/m. The ETA–C_{16}mimBr system also showed synergism in the presence of salt and maintained

an ultra-low IFT even at a high salinity of 15 wt% NaCl concentration. The IFT increased with the temperature due to the dissolved gases in crude oil.

The ETA–C_{16}mimBr combination also exhibited a synergistic performance in altering the surface of carbonate rock, while the effect of $NaBO_2$ on the wettability alteration capability of CTAB was not significant.

The emulsification studies confirmed the synergism in the IFT reduction performance of the AS formulations and showed that the ETA–C_{16}mimBr system could form very stable emulsions at high-temperature conditions just like the $NaBO_2$–CTAB system. Thus, this study showed that a combination of surface-active ionic liquid and organic alkali have excellent potential in enhancing the oil recovery in carbonate reservoirs at high-salinity, high-temperature conditions in carbonate formations.

Author Contributions: B.N.T.-O.: Conceptualization, Methodology, Writing—Original Draft; M.A.A.M.: Supervision, Funding acquisition, Writing—Review and Editing; H.A.B.M.Z.: Investigation; A.M.H.: Writing—Review and Editing; P.I.M.: Data curation, Writing—Original Draft; G.A.T.: Writing—Original Draft. All authors have read and agreed to the published version of the manuscript.

Funding: This research was funded by Universiti Teknologi Petronas through YUTP grant number [015LC0-105] And the APC was funded by [015LC0-105].

Institutional Review Board Statement: Not applicable.

Informed Consent Statement: Not applicable.

Data Availability Statement: Not applicable.

Acknowledgments: The authors wish to acknowledge the financial support from the Universiti Teknologi PATRONAS. The authors acknowledge the support of the Centre of Research in Enhanced Oil Recovery for making available most of the equipment used in the experiments.

Conflicts of Interest: The authors declare no conflict of interest.

Sample Availability: Samples are not available from the authors.

References

1. Mandal, A. Chemical flood enhanced oil recovery: A review. *Int. J. Oil Gas Coal Technol.* **2015**, *9*, 241. [CrossRef]
2. Gbadamosi, A.O.; Junin, R.; Manan, M.A.; Agi, A.; Yusuff, A.S. An overview of chemical enhanced oil recovery: Recent advances and prospects. *Int. Nano Lett.* **2019**, *9*, 171–202. [CrossRef]
3. Sheng, J. *Modern Chemical Enhanced Oil Recovery: Theory and Practice*; Gulf Professional Publishing: Houston, TX, USA, 2010.
4. Bera, A.; Belhaj, H. Application of nanotechnology by means of nanoparticles and nanodispersions in oil recovery—A comprehensive review. *J. Nat. Gas Sci. Eng.* **2016**, *34*, 1284–1309. [CrossRef]
5. Bera, A.; Shah, S.; Shah, M.; Agarwal, J.; Vij, R.K. Mechanistic study on silica nanoparticles-assisted guar gum polymer flooding for enhanced oil recovery in sandstone reservoirs. *Colloids Surfaces A Physicochem. Eng. Asp.* **2020**, *598*, 124833. [CrossRef]
6. Asl, H.F.; Zargar, G.; Manshad, A.K.; Takassi, M.A.; Ali, J.; Keshavarz, A. Effect of SiO_2 nanoparticles on the performance of L-Arg and L-Cys surfactants for enhanced oil recovery in carbonate porous media. *J. Mol. Liq.* **2020**, *300*, 112290. [CrossRef]
7. Zargar, G.; Arabpour, T.; Manshad, A.K.; Ali, J.A.; Sajadi, S.M.; Keshavarz, A.; Mohammadi, A.H. Experimental investigation of the effect of green TiO_2/quartz nanocomposite on interfacial tension reduction, wettability alteration, and oil recovery improvement. *Fuel* **2020**, *263*, 116599. [CrossRef]
8. Yekeen, N.; Manan, M.A.; Idris, A.K.; Samin, A.M.; Risal, A.R. Experimental investigation of minimization in surfactant adsorption and improvement in surfactant-foam stability in presence of silicon dioxide and aluminum oxide nanoparticles. *J. Pet. Sci. Eng.* **2017**, *159*, 115–134. [CrossRef]
9. Tackie-Otoo, B.N.; Mohammed, M.A.A.; Yekeen, N.; Negash, B.M. Alternative chemical agents for alkalis, surfactants and polymers for enhanced oil recovery: Research trend and prospects. *J. Pet. Sci. Eng.* **2020**, *187*, 106828. [CrossRef]
10. Zhao, F.; Ma, Y.; Hou, J.; Tang, J.; Xie, D. Feasibility and mechanism of compound flooding of high-temperature reservoirs using organic alkali. *J. Pet. Sci. Eng.* **2015**, *135*, 88–100. [CrossRef]
11. Berger, P.D.; Lee, C.H. Improved ASP process using organic alkali. In Proceedings of the SPE/DOE Symposium on Improved Oil Recovery, Tulsa, OK, USA, 11–13 April 2006; pp. 1–9.
12. Xie, D.; Hou, J.; Zhao, F.; Doda, A.; Trivedi, J. The comparison study of IFT and consumption behaviors between organic alkali and inorganic alkali. *J. Pet. Sci. Eng.* **2016**, *147*, 528–535. [CrossRef]

13. Xie, D.; Hou, J.; Doda, A.; Trivedi, J. Application of organic alkali for heavy-oil Enhanced Oil Recovery (EOR), in comparison with inorganic alkali. *Energy Fuels* **2016**, *30*, 4583–4595. [CrossRef]
14. Negin, C.; Ali, S.; Xie, Q. Most common surfactants employed in chemical enhanced oil recovery. *Petroleum* **2017**, *3*, 197–211. [CrossRef]
15. Xie, D.; Hou, J.; Doda, A.; Trivedi, J.J. Organic alkali for heavy oil chemical EOR improves the performance over inorganic alkali. In Proceedings of the Society of Petroleum Engineers—SPE International Heavy Oil Conference and Exhibition 2014: Heavy Oil Innovations Beyond Limitations, Mangaf, Kuwait, 8–10 December 2014; pp. 401–416.
16. Bai, Y.; Xiong, C.; Shang, X.; Xin, Y. Experimental study on ethanolamine/surfactant flooding for enhanced oil recovery. *Energy Fuels* **2014**, *28*, 1829–1837. [CrossRef]
17. Bai, Y.; Wang, Z.; Shang, X.; Dong, C.; Zhao, X.; Liu, P. Experimental evaluation of a surfactant/compound organic alkalis flooding system for enhanced oil recovery. *Energy Fuels* **2017**, *31*, 5860–5869. [CrossRef]
18. Takassi, M.A.; Hashemi, A.; Rostami, A. A lysine amino acid-based surfactant: Application in enhanced oil recovery A lysine amino acid-based surfactant: Application in enhanced oil recovery. *Pet. Sci. Technol.* **2016**, *34*, 1521–1526. [CrossRef]
19. Takassi, M.A.; Zargar, G.; Madani, M.; Zadehnazari, A. The preparation of an amino acid-based surfactant and its potential application as an EOR agent. *Pet. Sci. Technol.* **2017**, *35*, 385–391. [CrossRef]
20. Rostami, A.; Hashemi, A.; Takassi, M.A.; Zadehnazari, A. Experimental assessment of a lysine derivative surfactant for enhanced oil recovery in carbonate rocks: Mechanistic and core displacement analysis. *J. Mol. Liq.* **2017**, *232*, 310–318. [CrossRef]
21. Saxena, N.; Pal, N.; Dey, S.; Mandal, A. Characterizations of surfactant synthesized from palm oil and its application in enhanced oil recovery. *J. Taiwan Inst. Chem. Eng.* **2017**, *81*, 343–355. [CrossRef]
22. Pal, N.; Saxena, N.; Laxmi, K.D.; Mandal, A. Interfacial behaviour, wettability alteration and emulsification characteristics of a novel surfactant: Implications for enhanced oil recovery. *Chem. Eng. Sci.* **2018**, *187*, 200–212. [CrossRef]
23. Saxena, N.; Goswami, A.; Dhodapkar, P.K.; Nihalani, M.C.; Mandal, A. Bio-based surfactant for enhanced oil recovery: Interfacial properties, emulsification and rock-fluid interactions. *J. Pet. Sci. Eng.* **2019**, *176*, 299–311. [CrossRef]
24. Madani, M.; Zargar, G.; Takassi, M.A.; Daryasafar, A.; Wood, D.; Zhang, Z. Fundamental investigation of an environmentally-friendly surfactant agent for chemical enhanced oil recovery. *Fuel* **2019**, *238*, 186–197. [CrossRef]
25. Asl, H.F.; Zargar, G.; Manshad, A.K.; Takassi, M.A.; Ali, J.A.; Keshavarz, A. Experimental investigation into l-Arg and l-Cys eco-friendly surfactants in enhanced oil recovery by considering IFT reduction and wettability alteration. *Pet. Sci.* **2020**, *17*, 105–117. [CrossRef]
26. Tackie-Otoo, B.N.; Mohammed, M.A.A. Experimental investigation of the behaviour of a novel amino acid-based surfactant relevant to EOR application. *J. Mol. Liq.* **2020**, *316*, 113848. [CrossRef]
27. Machale, J.; Al-Bayati, D.; Almobarak, M.; Ghasemi, M.; Saeedi, A.; Sen, T.K.; Majumder, S.K.; Ghosh, P. Interfacial, emulsifying, and rheological properties of an additive of a natural surfactant and polymer and its performance assessment for application in enhanced oil recovery. *Energy Fuels* **2021**, *35*, 4823–4834. [CrossRef]
28. Bera, A.; Belhaj, H. Ionic liquids as alternatives of surfactants in enhanced oil recovery—A state-of-the-art review. *J. Mol. Liq.* **2016**, *224*, 177–188. [CrossRef]
29. Bera, A.; Agarwal, J.; Shah, M.; Shah, S.; Vij, R.K. Recent advances in ionic liquids as alternative to surfactants/chemicals for application in upstream oil industry. *J. Ind. Eng. Chem.* **2020**, *82*, 17–30. [CrossRef]
30. Kokal, S.; Al-Kaabi, A. *Enhanced oil recovery: Challenges and Opportunities*; Official Publication; World Petroleum Council: London, UK, 2010; pp. 64–69.
31. Akbar, M.; Vissapragada, B.; Alghamdi, A.H.; Allen, D.; Herron, M.; Carnegie, A.; Chourasiya, R.D.; Netherwood, R.; Russel, S.D.; Saxena, K. A snapshot of carbonate reservoir evaluation. *Oilfield Rev.* **2000**, *12*, 20–21.
32. Roehl, P.O.; Choquette, P.W. *Carbonate Petroleum Réservoirs*; Springer Science and Business Media: Berlin, Germany, 2012.
33. Standnes, D.C.; Austad, T. Wettability alteration in chalk: 2. Mechanism for wettability alteration from oil-wet to water-wet using surfactants. *J. Pet. Sci. Eng.* **2000**, *28*, 123–143. [CrossRef]
34. Olajire, A.A. Review of ASP EOR (Alkaline Surfactant Polymer Enhanced Oil Recovery) technology in the petroleum industry: Prospects and challenges. *Energy* **2014**, *77*, 963–982. [CrossRef]
35. Panthi, K.; Sharma, H.; Mohanty, K.K. ASP flood of a viscous oil in a carbonate rock. *Fuel* **2016**, *164*, 18–27. [CrossRef]
36. Sharma, H.; Dufour, S.; Arachchilage, G.W.P.; Weerasooriya, U.; Pope, G.A.; Mohanty, K. Alternative alkalis for ASP flooding in anhydrite containing oil reservoirs. *Fuel* **2015**, *140*, 407–420. [CrossRef]
37. Nandwani, S.K.; Malek, N.I.; Lad, V.N.; Chakraborty, M.; Gupta, S. Study on interfacial properties of Imidazolium ionic liquids as surfactant and their application in enhanced oil recovery. *Colloids Surf. A Physicochem. Eng. Asp.* **2017**, *516*, 383–393. [CrossRef]
38. Bajani, D.; Gharai, D.; Dey, J. A comparison of the self-assembly behaviour of sodium N-lauroyl sarcosinate and sodium N-lauroyl glycinate surfactants in aqueous and aqueo-organic media. *J. Colloid Interface Sci.* **2018**, *529*, 314–324. [CrossRef] [PubMed]
39. Roy, S.; Dey, J. Self-organization properties and microstructures of sodium N-(11-Acrylamidoundecanoyl)-L-valinate and -L-threoninate in water. *Bull. Chem. Soc. Jpn.* **2006**, *79*, 59–66. [CrossRef]
40. Rosen, M.J.; Kunjappu, J.T. *Surfactants and Interfacial Phenomena*; John Wiley & Sons: Hoboken, NJ, USA, 2012; Volume 82, p. 336337.
41. Wintgens, V.; Harangozó, J.G.; Miskolczy, Z.; Guigner, J.-M.; Amiel, C.; Biczók, L. Effect of headgroup variation on the self-assembly of cationic surfactants with sulfonatocalix[6]arene. *Langmuir* **2017**, *33*, 8052–8061. [CrossRef] [PubMed]

42. Rodríguez-Escontrela, I.; Rodríguez-Palmeiro, I.; Rodríguez, O.; Arce, A.; Soto, A. Characterization and phase behavior of the surfactant ionic liquid tributylmethylphosphonium dodecylsulfate for enhanced oil recovery. *Fluid Phase Equilibria* **2016**, *417*, 87–95. [CrossRef]
43. Gad, E.A.M.; El-Sukkary, M.M.A.; Ismail, D.A. Surface and thermodynamic parameters of sodium N-acyl sarcosinate surfactant solutions. *J. Am. Oil Chem. Soc.* **1997**, *74*, 43–47. [CrossRef]
44. Yoshimura, T.; Akiba, K. Solution properties of dissymmetric sulfonate-type anionic Gemini surfactants. *J. Oleo Sci.* **2016**, *65*, 135–141. [CrossRef] [PubMed]
45. Sugihara, G.; Miyazono, A.; Nagadome, S.; Oida, T.; Hayashi, Y.; Ko, J.-S. Adsorption and micelle formation of mixed surfactant systems in water II: A combination of cationic Gemini-type surfactant with MEGA-10. *J. Oleo Sci.* **2003**, *52*, 449–461. [CrossRef]
46. Williams, R.J.; Phillips, J.N.; Mysels, K.J. The critical micelle concentration of sodium lauryl sulphate at 25 °C. *Trans. Faraday Soc.* **1955**, *51*, 728–737. [CrossRef]
47. Mukerjee, P.; Mysels, K. *Critical Micelle Concentrations of Aqueous Surfactant Systems. National Standard Reference Data System*; NBS Publications: Swindon, UK, 1971. [CrossRef]
48. Zana, R. Critical micellization concentration of surfactants in aqueous solution and free energy of micellization. *Langmuir* **1996**, *12*, 1208–1211. [CrossRef]
49. Ray, G.B.; Ghosh, S.; Moulik, S.P. Physicochemical studies on the interfacial and bulk behaviors of Sodium N-Dodecanoyl Sarcosinate (SDDS). *J. Surfactants Deterg.* **2009**, *12*, 131–143. [CrossRef]
50. Zhang, Y.; You, Q.; Fu, Y.; Zhao, M.; Fan, H.; Liu, Y.; Dai, C. Investigation on interfacial/surface properties of bio-based surfactant N-aliphatic amide-N, N-diethoxypropylsulfonate sodium as an oil displacement agent regenerated from waste cooking oil. *J. Mol. Liq.* **2016**, *223*, 68–74. [CrossRef]
51. Bunge, A.L.; Radke, C.J. Divalent ion exchange with alkali. *Soc. Pet. Eng. J.* **1983**, *23*, 657–668. [CrossRef]
52. Krumrine, P.; Mayer, E.H.; Brock, G.F. Scale formation during alkaline flooding. *J. Pet. Technol.* **1985**, *37*, 1–466. [CrossRef]
53. Lo, S.-W.; Shahin, G.T.; Graham, G.M.; Simpson, C.; Kidd, S. Scale control and inhibitor evaluation of an alkaline surfactant polymer flood. In Proceedings of the SPE International Symposium on Oilfield Chemistry, The Woodlands, TX, USA, 11–13 April 2011. [CrossRef]
54. Stellner, K.L.; Scamehorn, J.F. Hardness tolerance of anionic surfactant solutions. 2. Effect of added nonionic surfactant. *Langmuir* **1989**, *5*, 77–84. [CrossRef]
55. Guerra, E.; Valero, E.M.; Rodriquez, D.; Gutierrez, L.; Castillo, M.; Espinoza, J.; Granja, G. Improved ASP design using organic compound-surfactant-polymer (OCSP) for La Salina Field, Maracaibo Lake. In Proceedings of the Latin American and Caribbean Petroleum Engineering Conference, Buenos Aires, Argentina, 15–18 April 2007.
56. Walter, K. Complex Compound of Alkali-and Alkaline Earth-Metal Halides. U.S. Patent 717,267A, 22 October 1935.
57. Zhang, J.; Nguyen, Q.P.; Flaaten, A.; Pope, G.A. Mechanisms of enhanced natural imbibition with novel chemicals. *SPE Reserv. Eval. Eng.* **2009**, *12*, 912–920. [CrossRef]
58. Flaaten, A.; Nguyen, Q.P.; Pope, G.A.; Zhang, J. A systematic laboratory approach to low-cost, high-performance chemical flooding. In Proceedings of the SPE Symposium on Improved Oil Recovery, Tulsa, OK, USA, 20–23 April 2008; Society of Petroleum Engineers: Richardson, TX, USA, 2008; p. 20.
59. Yang, P.; Li, Z.A.; Xia, B.; Yuan, Y.J.; Huang, Q.T.; Liu, W.L.; Cheng, C.Y. Comprehensive review of Alkaline–Surfactant–Polymer (ASP)-Enhanced Oil Recovery (EOR). In *Proceedings of the 2017 International Field Exploration and Development Conference*; Springer: Singapore, 2019; pp. 858–872.
60. Sheng, J. A comprehensive review of Alkaline-Surfactant-Polymer (ASP) flooding. In Proceedings of the SPE Western Regional & AAPG Pacific Section Meeting 2013 Joint Technical Conference, Monterey, CA, USA, 19–25 April 2013. [CrossRef]
61. Kumar, S.; Mandal, A. Studies on interfacial behavior and wettability change phenomena by ionic and nonionic surfactants in presence of alkalis and salt for enhanced oil recovery. *Appl. Surf. Sci.* **2016**, *372*, 42–51. [CrossRef]
62. Sun, J.; Sun, L.; Liu, W.; Liu, X.; Li, X.; Shen, Q. Alkaline consumption mechanisms by crude oil: A comparison of sodium carbonate and sodium hydroxide. *Colloids Surfaces A Physicochem. Eng. Asp.* **2008**, *315*, 38–43. [CrossRef]
63. Gong, H.; Li, Y.; Dong, M.; Zhu, T.; Yu, L. Enhanced heavy oil recovery by organic alkali combinational flooding solutions. *J. Dispers. Sci. Technol.* **2017**, *38*, 551–557. [CrossRef]
64. Hanamertani, A.S.; Pilus, R.M.; Irawan, S. A review on the application of ionic liquids for enhanced oil recovery. In Proceedings of the International Conference on Integrated Petroleum Engineering and Geosciences (ICIPEG 2016), Kuala Lumpur, Malaysia, 15–17 August 2016; Springer: Singapore, 2017; pp. 133–147.
65. Pillai, P.; Kumar, A.; Mandal, A. Mechanistic studies of enhanced oil recovery by imidazolium-based ionic liquids as novel surfactants. *J. Ind. Eng. Chem.* **2018**, *63*, 262–274. [CrossRef]
66. Karnanda, W.; Benzagouta, M.S.; AlQuraishi, A.; Amro, M.M. Effect of temperature, pressure, salinity, and surfactant concentration on IFT for surfactant flooding optimization. *Arab. J. Geosci.* **2013**, *6*, 3535–3544. [CrossRef]
67. Okasha, T. Investigation of the effect of temperature and pressure on interfacial tension and wettability. In Proceedings of the International Symposium of the Society of Core Analysts, Trondheim, Norway, 27–30 August 2018.
68. Muggeridge, A.; Cockin, A.; Webb, K.; Frampton, H.; Collins, I.; Moulds, T.; Salino, P. Recovery rates, enhanced oil recovery and technological limits. *Philos. Trans. R. Soc. London. Ser. A Math. Phys. Eng. Sci.* **2014**, *372*, 20120320. [CrossRef] [PubMed]

69. Bennett, B.; Buckman, J.O.; Bowler, B.F.J.; Larter, S.R. Wettability alteration in petroleum systems: The role of polar non-hydrocarbons. *Pet. Geosci.* **2004**, *10*, 271–277. [CrossRef]
70. Deng, X.; Kamal, M.S.; Patil, S.; Hussain, S.M.S.; Zhou, X. A review on wettability alteration in carbonate rocks: Wettability modifiers. *Energy Fuels* **2019**, *34*, 31–54. [CrossRef]
71. Reisberg, J.; Doscher, T.M. Interfacial phenomena in crude oil-water systems. *Prod. Mon.* **1956**, *21*, 43–50.
72. Ehrlich, R.; Hasiba, H.; Raimondi, P. Alkaline waterflooding for wettability alteration-evaluating a potential field application. *J. Pet. Technol.* **1974**, *26*, 1335–1343. [CrossRef]
73. Tackie-Otoo, B.N.; Atta, D.Y.; Mohammed, M.A.A.; Otchere, D.A. Investigation into the oil recovery process using an organic alkali–amino acid-based surfactant system. *Energy Fuels* **2021**, *35*, 11171–11192. [CrossRef]
74. Zhang, D.L.; Liu, S.; Puerto, M.; Miller, C.A.; Hirasaki, G.J. Wettability alteration and spontaneous imbibition in oil-wet carbonate formations. *J. Pet. Sci. Eng.* **2006**, *52*, 213–226. [CrossRef]
75. Li, J.; Wang, W.; Gu, Y. Dynamic interfacial tension phenomenon and wettability alteration of crude oil-rock-alkaline-surfactant solution systems. In Proceedings of the SPE Annual Technical Conference and Exhibition, Houston, TX, USA, 26–29 September 2004; pp. 1803–1811. [CrossRef]
76. Dehghan, A.A.; Masihi, M.; Ayatollahi, S. Interfacial tension and wettability change phenomena during alkali–surfactant interactions with acidic heavy crude oil. *Energy Fuels* **2015**, *29*, 649–658. [CrossRef]
77. Biswas, A.K.; Mukherji, B.K. Influence of additives on the properties of surfactant solutions. *J. Appl. Chem.* **1960**, *10*, 73–80. [CrossRef]
78. Rosen, M.J.; Zhu, Z.H. Enhancement of wetting properties of water-insoluble surfactants via solubilization. *J. Am. Oil Chem. Soc.* **1993**, *70*, 65–68. [CrossRef]
79. Bryan, J.; Kantzas, A. Potential for alkali-surfactant flooding in heavy oil reservoirs through oil-in-water emulsification. *J. Can. Pet. Technol.* **2009**, *48*, 37–46. [CrossRef]
80. Kokal, S.L. Crude oil emulsions: A state-of-the-art review. *SPE Prod. Facil.* **2005**, *20*, 5–13. [CrossRef]
81. Scott, G.; Collins, H.; Flock, D. Improving waterflood recovery of viscous crude oils by chemical control. *J. Can. Pet. Technol.* **1965**, *4*, 243–251. [CrossRef]
82. Mohamed, A.I.A.; Sultan, A.S.; Hussein, I.A.; Al-Muntasheri, G.A. Influence of surfactant structure on the stability of water-in-oil emulsions under high-temperature high-salinity conditions. *J. Chem.* **2017**, *2017*, 5471376. [CrossRef]